Earth Surf. Dynam., 14, 211–231, 2026
https://doi.org/10.5194/esurf-14-211-2026

Earth Surface Dynamics
Open Access
EGU

Discriminating fluvial fans and deltas: channel network morphometrics reflect distinct formative processes

Luke Gezovich[1], Piret Plink-Björklund[1], and Jack Henry[1,2]

[1]Colorado School of Mines, Geology & Geologic Engineering, 1500 Illinois Street, Golden, CO 80401, USA
[2]Rice University, Earth, Environmental and Planetary Sciences, 6100 Main St., Houston, TX 77005-1827, USA

Correspondence: Luke Gezovich (lukegezovich@mines.edu)

Received: 28 May 2025 – Discussion started: 10 July 2025
Revised: 28 September 2025 – Accepted: 19 October 2025 – Published: 17 March 2026

Abstract. Recent recognition of a new type of fluvial system – fluvial fans – introduces a fan-shaped channel network that appears similar to that of river-dominated deltas. Deltas form where rivers enter lakes and oceans, while fluvial fans are terrestrial landforms. However, fluvial fans can reach the shorelines of oceans or lakes, and in such cases the distinction between fluvial fan and river-dominated delta channel networks becomes ambiguous. We currently lack fundamental understanding of these two landforms' morphometric differences, despite their high socioeconomic significance, vulnerability to natural hazards, and key differences in how these landforms respond to global climate change and urbanization. Here we review the relevant conceptual differences in delta and fluvial fan network morphodynamics, propose a set of quantitative morphometric criteria to distinguish fluvial fan and delta channel networks, and test these criteria on 40 deltas and 40 fluvial fans from across the world. This initial attempt to contrast and distinguish deltas and fluvial fans based on their channel network morphometrics demonstrates that quantifying channel network angles (mean of 74.0° for deltas and 55.0° for fluvial fans) and trends in normalized channel widths and lengths provide efficient criteria, but some ambiguities remain that need to be resolved in future work. This research advances our mechanistic understanding of fluvial fan and delta channel networks and the recognition of modern and ancient landforms on Earth and other planetary bodies, such as Mars and Saturn's moon Titan.

1 Introduction

River deltas are depositional landforms that form where rivers enter lakes or oceans. They are home to over half a billion people, host abundant and biodiverse ecosystems, and function as both economic and agricultural hubs (Saito et al., 2007; Tejedor et al., 2015). Deltas are global change hotspots highly vulnerable to urbanization and climate change, which can aggravate coastal hazards and cause sea-level rise (Giosan et al., 2014; Syvitski et al., 2009), and reduce sediment supply due to river damming and artificial levees causing the drowning of deltas (Blum and Roberts, 2009; Giosan et al., 2014; Nienhuis et al., 2020; Paola et al., 2011; Syvitski et al., 2009). The form and function of deltas is intimately linked to the evolving structure of their channel networks that determine how deltas distribute sediment and nutrients (Passalacqua, 2017; Pearson et al., 2020; Tejedor et al., 2017). Delta channel network morphology results from an intricate balance between sediment erosion and deposition from river, tide, and wave energy fluxes. River fluxes create distributary channels and islands, tides roughen the shoreline and widen the channels, and waves smooth the shoreline and decrease the number of distributary channels (Broaddus et al., 2022; Galloway, 1975; Nienhuis et al., 2015, 2018; Paniagua-Arroyave and Nienhuis, 2024; Vulis et al., 2023). Deltas dominated by river energy fluxes (river-dominated deltas) (Broaddus et al., 2022; Galloway, 1975; Nienhuis et al., 2015, 2018; Paniagua-Arroyave and Nienhuis, 2024; Vulis et al., 2023) characteristically form fan-shaped landforms with complex distributary channel networks (Fig. 1). In these deltas, channel network topology is defined by mouth bar deposition and consequent distributary

channel bifurcation (Bates, 1953; Edmonds and Slingerland, 2007; Wright, 1977).

Fluvial fans are another type of fan-shaped landform with channel networks that share morphological similarities with river-dominated delta channel networks (Fig. 2). Fluvial fans are a relatively newly acknowledged type of fluvial landform (Ventra and Clarke, 2018; Weissmann et al., 2010), which forms via river avulsions or "channel jumps" across low-gradient floodplains (Chakraborty et al., 2010; Martin and Edmonds, 2023; North and Warwick, 2007). Rivers have been traditionally regarded as sediment transfer or bypass zones in source-to-sink systems (Allen, 2008; Fielding et al., 2012), whereas fluvial fans are net depositional and build significant stratigraphic thicknesses (Chakraborty et al., 2010; Moscariello, 2018; Weissmann et al., 2015). Fluvial fans are also called "wet" fluvial-dominated alluvial fans (Schumm, 1977), megafans (Singh et al., 1993), or distributive fluvial systems (DFS) (Weissmann et al., 2010). Fluvial fans are distinct landforms from alluvial fans – which form by a combination of gravitational and streamflow processes, feature steep gradients (typically 2–12°), and have a relatively small radius typically less than 10 km (Blair and McPherson, 1994; Moscariello, 2018). Fluvial fans form some of the largest terrestrial landforms on Earth (10^3–10^5 km^2 in surface area) (Horton and DeCelles, 2001; Leier et al., 2005) and have low gradients (0.0018–1.5°) (Hartley et al., 2010). Fluvial fans are abundant across Earth, and they form in diverse climatic and tectonic settings (Hartley et al., 2010; Ventra and Clarke, 2018; Weissmann et al., 2010).

Like deltas, fluvial fans are home to hundreds of millions of people, and these highly dynamic landforms are critical for their livelihood – supporting agriculture, fisheries, and freshwater access. They also experience catastrophic floods; for example, the Kosi fluvial fan floods have led to large numbers of casualties and displaced populations (Sinha, 2009; Syvitski and Brakenridge, 2013). While fluvial fans are terrestrial landforms, they can reach the shorelines of oceans (Fig. 2b) or lakes (Fig. 2a, d, and i). In such cases the distinction between fluvial fan and river-dominated delta channel networks becomes ambiguous, while wave- and tide-dominated deltas have distinctly recognizable morphologies (Broaddus et al., 2022; Galloway, 1975; Nienhuis et al., 2015, 2018; Paniagua-Arroyave and Nienhuis, 2024; Vulis et al., 2023). We currently lack quantitative morphometric criteria for distinguishing river-dominated delta and fluvial fan channel networks, despite their socioeconomic significance, key differences in their natural hazard vulnerabilities, and in how they respond to global change.

Numerous fan-shaped landforms with channel networks have also been identified on other planetary bodies such as Mars (Malin and Edgett, 2015; Ori et al., 2000; Wood, 2006) and Saturn's moon Titan (Radebaugh et al., 2018; Wall et al., 2010; Witek and Czechowski, 2015). Deltas on planetary bodies are important indicators of paleo-shorelines and have been utilized to reconstruct the shorelines and water levels of ancient lakes and oceans on Mars (Di Achille and Hynek, 2010). However, Martian paleo-ocean shoreline reconstructions have so far yielded mixed results (De Toffoli et al., 2021). This discrepancy could perhaps arise because shoreline-bound deltas have not been effectively distinguished from fluvial fans on Mars, which may form thousands of kilometers inland from shorelines (Bramble et al., 2019; Limaye et al., 2023; Tebolt and Goudge, 2022). Deltas also offer attractive targets for mission sites in search of life due to their habitability and high biosignature preservation potential, as exemplified by the selection of Jezero Crater for NASA's *Perseverance* rover, *Ingenuity* helicopter, and future Mars Sample Return mission (Farley et al., 2020). Distinguishing deltaic and fluvial fan paleo-channel networks on other planetary bodies is even more ambiguous, especially if the lakes and oceans are no longer present.

Over time, the accumulation of biogenic and sedimentary materials distributed via channel networks contributes to the construction of stratigraphy. Fluvial fans and deltas are both net depositional systems characterized by spatially diminishing water surface slopes that reduce sediment transport capacity, thereby producing spatiotemporal convergence and deposition of sediment (Ganti et al., 2014). Consequently, in addition to their socioeconomic significance, both landforms significantly contribute to the stratigraphic record, and their deposits can be used to decipher past environmental conditions. High deposition rates in fluvial fans and deltas promote the preservation of environmental change signals in the sedimentary record (Trampush and Hajek, 2017). Similar to modern river-dominated deltas and fluvial fans, we lack morphometric criteria to distinguish these two fan-shaped channel networks in the sedimentary record, such as in seismic datasets.

This study is motivated by developing quantitative morphometric distinction criteria for fluvial fan and river-dominated delta channel networks. Prior work has established quantitative morphological criteria for describing deltaic channel networks and linked these characteristics to theory (Chen et al., 2021; Coffey and Shaw, 2017; Edmonds et al., 2011; Edmonds and Slingerland, 2007; Fagherazzi et al., 2015; Ke et al., 2019; Passalacqua, 2017; Pearson et al., 2020; Tejedor et al., 2015, 2017). However, there are no existing quantitative criteria to characterize fluvial fan channel networks or to differentiate the two landforms. To develop such criteria, we review the relevant conceptual differences in delta and fluvial fan network morphodynamics, propose quantitative morphometric criteria to distinguish fluvial fan and delta channel networks, and test these criteria on 40 deltas and 40 fluvial fans (the Supplement) from across the globe (Fig. 3). We test the robustness of the approach by analyzing differences in channel network morphometrics concerning the size and gradient of the systems, lake versus ocean terminations and tide versus wave influences in deltas, and fan termination styles in fluvial fans. We assess how effectively the proposed methods distinguish fluvial fans from

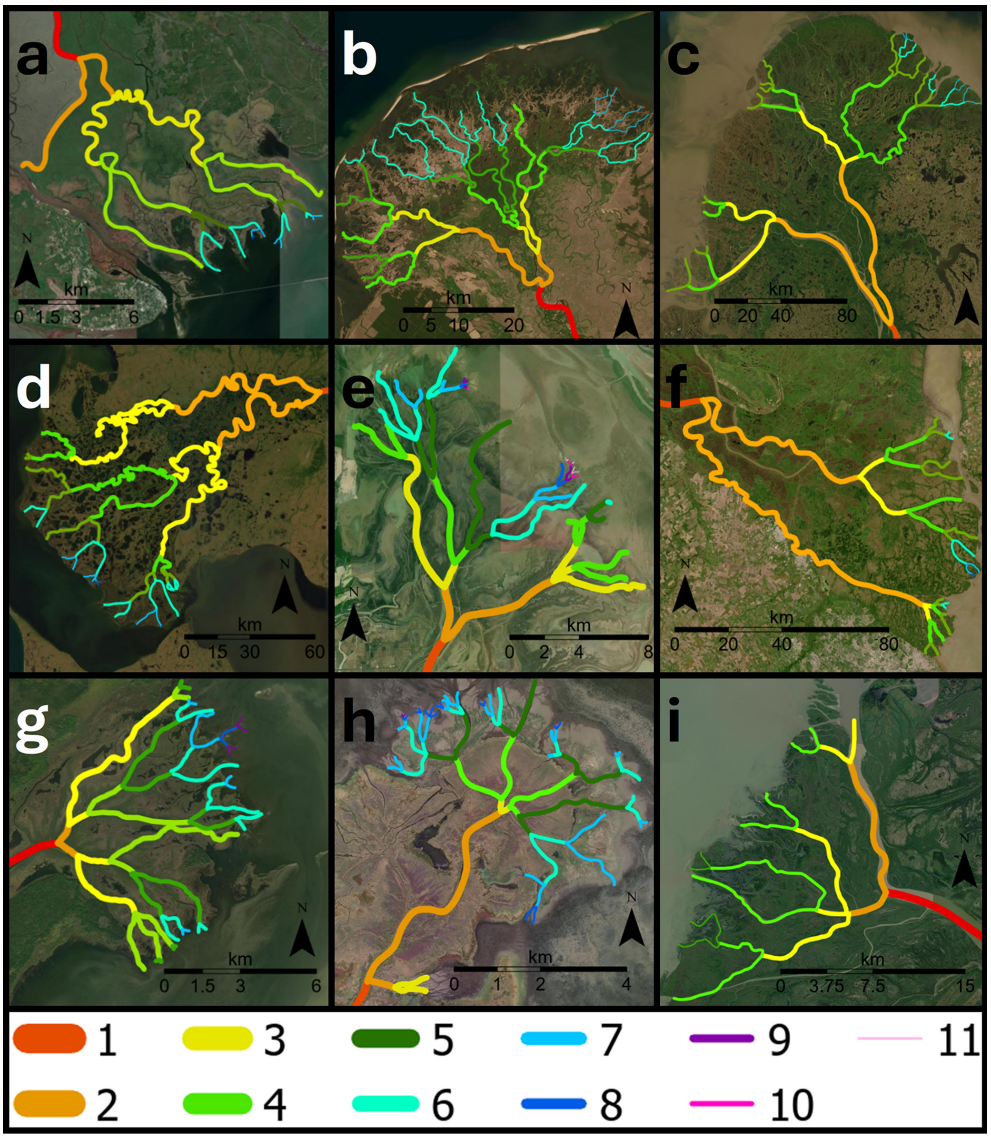

Figure 1. Examples of delta channel networks: **(a)** Apalachicola, **(b)** Selenga, **(c)** Yukon, **(d)** Kobuk, **(e)** Poyang Lake, **(f)** Parana, (g) Saskatchewan, **(h)** Mamawi lake, **(i)** Slave deltas. The colors indicate channel hierarchy (see Methods). Base imagery from Esri's World Imagery basemap (© Esri, DigitalGlobe, GeoEye, i-cubed, USDA FSA, USGS, AEX, Getmapping, Aerogrid, IGN, IGP, swisstopo, and the GIS User Community). Colors and relative line thicknesses indicate channel hierarchy (see Methods), with the widest lines representing order 1 channels and progressively thinner lines representing higher channel orders.

river-dominated deltas and examine why this distinction matters under global change. This work serves to improve our mechanistic understanding of fluvial fan and delta evolution, and their accurate recognition on Earth, other planetary bodies, and in the sedimentary record.

2 Delta and Fluvial Fan Channel Network Morphodynamics

The nature of channel networks is dependent on distinct morphodynamic processes responsible for their formation (Edmonds and Slingerland, 2007; Fagherazzi et al., 2015; Tejedor et al., 2015). Below we analyze differences in delta and fluvial fan morphodynamics and review existing morphometric criteria for quantifying deltaic distributary channel networks. Our review is not comprehensive; rather, it focuses on the specific processes that govern the formation of the morphometric characteristics that we can then use for distinction of these two landforms, namely channel network angles, and downstream changes in channel widths and lengths. There are other important characteristics of deltaic channel networks, linked to water and sediment discharge distribution, entropy, and connectivity (Chen et al., 2021; Ke et al., 2019; Passalacqua, 2017; Pearson et al., 2020; Tejedor et al., 2015,

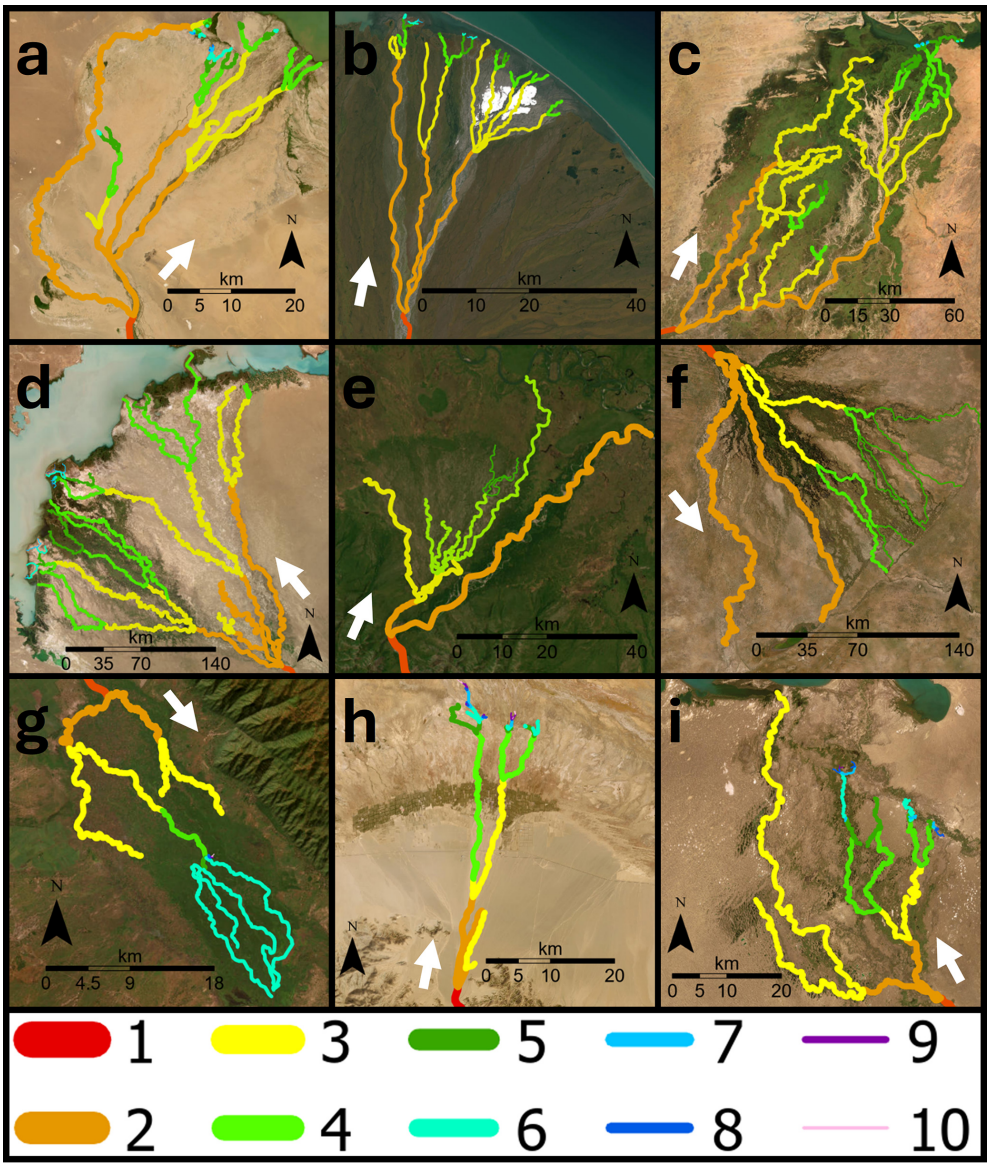

Figure 2. Examples of fluvial fan channel networks: **(a)** Dzavhan Gol, **(b)** Kongakut, **(c)** Niger, **(d)** Ili, **(e)** Bayunda, **(f)** Okavango, **(g)** Shire, **(h)** Nomon He, and **(i)** Aksu fans. The colors indicate channel hierarchy (see Methods), and white arrows indicates downfan direction. Base imagery from Esri's World Imagery basemap (© Esri, DigitalGlobe, GeoEye, i-cubed, USDA FSA, USGS, AEX, Getmapping, Aerogrid, IGN, IGP, swisstopo, and the GIS User Community). Colors and relative line thicknesses indicate channel hierarchy (see Methods), with the widest lines representing order 1 channels and progressively thinner lines representing higher channel orders.

2017). These aspects are not considered in this review, because they are outside the scope of this study that seeks to distinguish deltaic and fluvial fan channel networks using easily applicable morphometric criteria that can be used for both deltaic and fluvial fan networks.

2.1 River Deltas

Deltas (Fig. 1) form only where a river enters a standing body of water. Here, the transport capacity of the turbulent jet decreases, and the "parent" stream jet flow experiences both lateral and bed friction, causing the flow to decelerate and rapidly expand laterally (Bates, 1953; Edmonds and Slingerland, 2007; Jerolmack and Swenson, 2007; Wright, 1977). As a result, the transport capacity of the turbulent jet decreases and sediment is deposited as a mouth bar basinward of the river mouth (Edmonds and Slingerland, 2007). The process of mouth bar deposition and growth eventually leads to the downstream branching, or *bifurcation*, of a single (parent) channel into two daughter channels (Axelsson, 1967; Coffey and Shaw, 2017; Edmonds and Slingerland, 2007) (Fig. 4a). These daughter channels are separated by

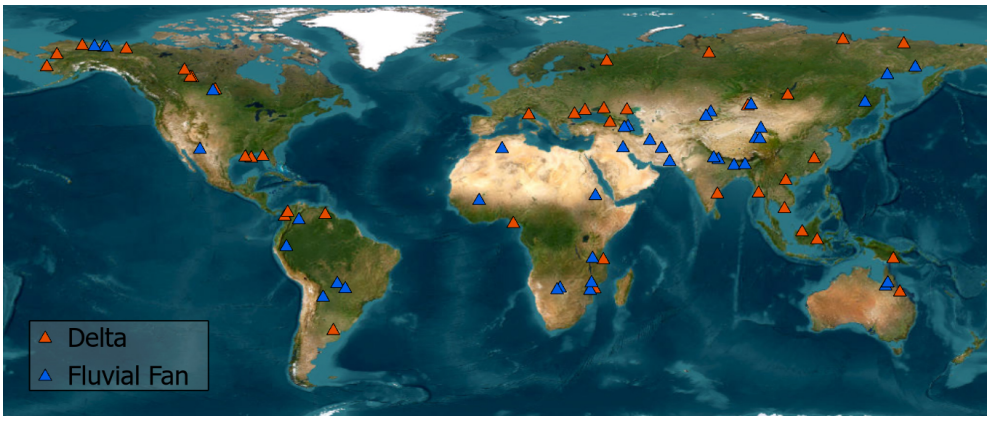

Figure 3. Map of deltas and fluvial fans in this study. Base imagery from Esri's World Imagery basemap (© Esri, DigitalGlobe, GeoEye, i-cubed, USDA FSA, USGS, AEX, Getmapping, Aerogrid, IGN, IGP, swisstopo, and the GIS User Community).

an island or shallow bay where sediment transport is significantly reduced or nonexistent, and flow is unchannelized (Coffey and Shaw, 2017). Mouth bar deposition and resultant channel bifurcation repeat multiple times, leading to the seaward advancement of the shoreline and the construction of a delta distributary channel network (Edmonds and Slingerland, 2007; Olariu and Bhattacharya, 2006) (Fig. 4a).

Deltas also experience channel avulsions or "channel jumps" at the lobe-level (Slingerland and Smith, 2004). These deltaic avulsions occur within a region of high-water surface slope variability caused by backwater hydrodynamics that are characterized by spatial flow deceleration and deposition during low flows, and flow acceleration and bed scour with high flows (Brooke et al., 2022; Chatanantavet et al., 2012; Chatanantavet and Lamb, 2014). As the backwater zone sets the location for avulsion in deltas (Chatanantavet et al., 2012), they are strongly controlled by hydrodynamics in their receiving basin, like mouth-bar-driven bifurcations. As a result, the delta lobe size is generally consistent and the lobe avulsion node migrates downstream commensurate with shoreline progradation (Ganti et al., 2014), as influenced by flood frequency, sediment supply, or sea-level rise (Brooke et al., 2022). These avulsions episodically rearrange the depocenter at the delta lobe scale, whereas the substantially more frequent mouth-bar-driven bifurcations generate the topology of the delta distributary channel networks (Bentley et al., 2016; Edmonds and Slingerland, 2007).

Resultant delta channel networks have a specific angle at which distributary channels bifurcate (Fig. 4b) (Coffey and Shaw, 2017), because a mouth-bar-driven bifurcation will grow toward an equilibrium angle of 72° to maximize flux at the two channel tips (Coffey and Shaw, 2017; Devauchelle et al., 2012; Ke et al., 2019; Mahon et al., 2024). First described in tributary networks, this theoretical angle arises from diffusive groundwater flow (Devauchelle et al., 2012). Testing of this concept reports mouth-bar-driven bifurcation angles of $70.4 \pm 2.6°$ ($n = 9$) in natural deltas (Coffey and Shaw, 2017), and $68.3 \pm 8.7°$ ($n = 21$) (Coffey and Shaw, 2017) and $74.1 \pm 7.7°$ ($n = 13$) (Federici and Paola, 2003) in experimental deltas.

Deltaic channel networks tend to consistently self-organize (Edmonds et al., 2011; Fagherazzi, 2008) and exhibit a theoretical fractal pattern of decreasing channel widths and lengths associated with increasing bifurcation order (Edmonds et al., 2011; Edmonds and Slingerland, 2007; Hariharan et al., 2022; Seybold et al., 2017; Wolinsky et al., 2010) (Fig. 4a). Edmonds and Slingerland (2007) show that channel width trends align with hydraulic geometric scaling: as the discharge of a parent channel divides into the discharge for two resultant daughter channels, the daughter channel dimensions decrease as they scale with bankfull discharge. Channel lengths decrease downstream with each successive bifurcation because the jet momentum flux and consequent average grain transport distance decrease downstream, causing new mouth bar deposition and accompanying bifurcations to occur closer to the previous bifurcation node for a given channel (Edmonds and Slingerland, 2007) (Fig. 4a, b).

The nature of delta channel networks is further affected by waves and tides (Broaddus et al., 2022; Geleynse et al., 2011; Jerolmack and Swenson, 2007) where the relative strength of river, wave, and tide processes determines whether deltas are river, wave, or tide dominated (Galloway, 1975; Nienhuis et al., 2015, 2018; Paniagua-Arroyave and Nienhuis, 2024; Vulis et al., 2023). Since wave- and tide-*dominated* deltas exhibit distinct morphologies from river-dominated delta and fluvial fan channel networks, they are not considered in this study (see Methods for more information on classification).

2.2 Fluvial Fans

Fluvial fans are fan-shaped landforms that form by river avulsions or "channel jumps" across a low-gradient floodplain (Chakraborty et al., 2010; Martin and Edmonds, 2023). In

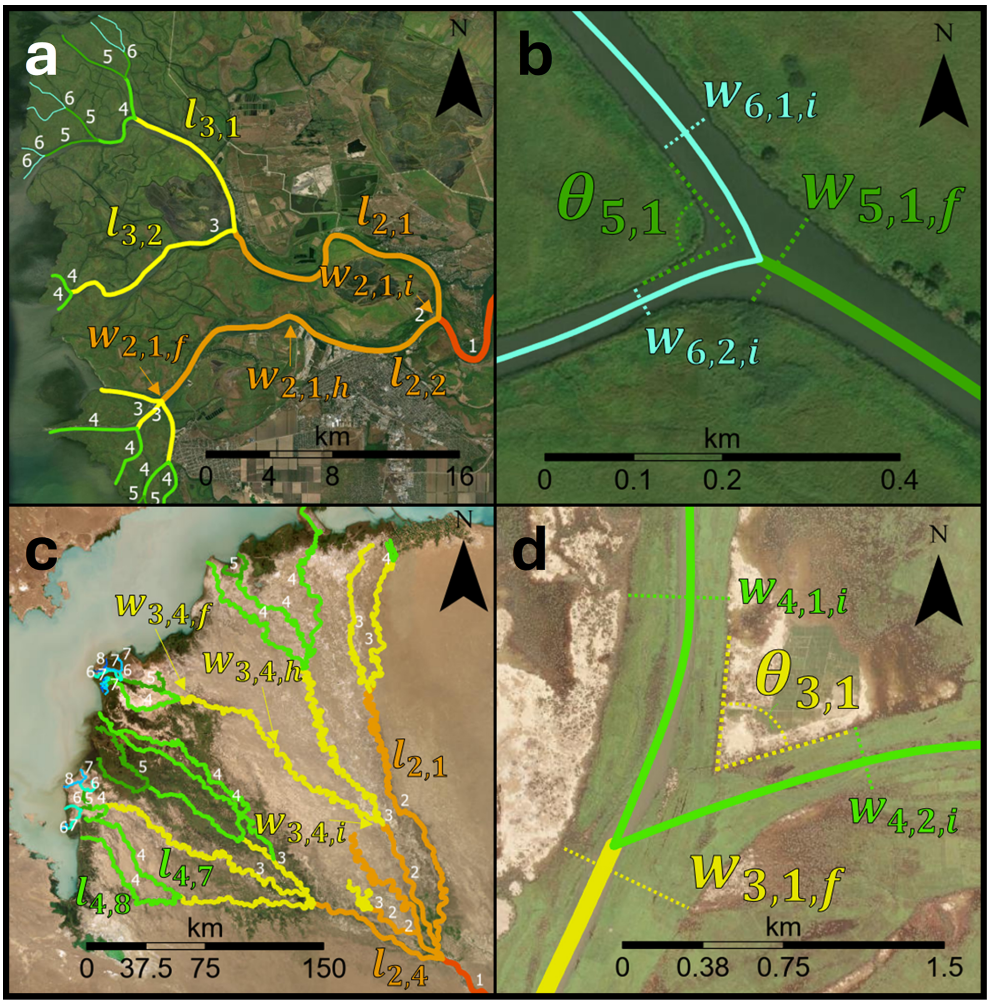

Figure 4. Illustration of **(a)** channel order, length, and width and **(b)** bifurcation angle measurements in deltas (Don delta). Illustration of **(c)** channel order, length, and width (Ili fan) and **(d)** divergence/crossover angle measurement (Niger fan). Arrows point to locations of w_i = initial channel width, w_h = midpoint channel width, w_f = final width measurements. The w_f is set as the length of two limbs that track along the edges of the mouth bar. θ_n corresponds to the bifurcation or divergence/crossover order. Base imagery from Esri's World Imagery basemap (© Esri, DigitalGlobe, GeoEye, i-cubed, USDA FSA, USGS, AEX, Getmapping, Aerogrid, IGN, IGP, swisstopo, and the GIS User Community).

contrast to deltas where mouth-bar-driven bifurcations and backwater-driven avulsions are strongly controlled by hydrodynamics near a receiving basin of standing water (Brooke et al., 2022; Chatanantavet et al., 2012; Ganti et al., 2014), *avulsions* that form fluvial fans are driven by a topographic slope break (Ganti et al., 2014; Martin and Edmonds, 2023). Increased likelihood of avulsions at the fan apex is a consequence of the gradient reduction that triggers in-channel sediment aggradation (Parker et al., 1998). These avulsions result from high channel bed aggradation rates that are considerably higher than on the surrounding floodplains (Pizzuto, 1987). Set up by in-channel aggradation, avulsions develop where a channel changes its course due to channel superelevation (Bryant et al., 1995; Gearon et al., 2024; Mohrig et al., 2000) or a more favorable (steeper) gradient at channel flanks (Gearon et al., 2024; Jones and Schumm, 1999; Slingerland and Smith, 2004). Since the slope break controls the location of the fluvial fan's apex, this avulsion node is topographically pinned at this change in gradient, unlike in deltas (Ganti et al., 2014; Brooke et al., 2022). Partial or full avulsions also occur further downfan, involving local gradient or discharge decreases, or crevassing processes (Assine, 2005; Chakraborty et al., 2010; Donselaar et al., 2013; Gearon et al., 2024) (Fig. 2).

Fluvial fan channel networks thus result through repeated nodal style avulsions (Slingerland and Smith, 2004) that typically shift the primary river to different regions of the fan (Chakraborty et al., 2010; Martin and Edmonds, 2023; North and Warwick, 2007). These avulsions superimpose new channel positions on paleo-channel locations and can split

channels by partial avulsions and crevasses. This generates channel and paleo-channel branching formed by processes distinct from deltas (North and Warwick, 2007) (Fig. 4c, d), where channel branching is predominantly caused by mouth-bar-driven bifurcations. In fluvial fans, channel branching is related to avulsions, which generate channel networks that are predominantly paleo-channel networks rather than active channel networks like in deltas (Chakraborty et al., 2010; North and Warwick, 2007). Multiple channels can actively transmit discharge at partial avulsions, such as during major river floods.

Downfan decreases in channel width have been well documented in modern and ancient fluvial fans (Davidson et al., 2013; Kelly and Olsen, 1993; Nichols, 1987; Nichols and Fisher, 2007; Owen et al., 2015; Wang and Plink-Björklund, 2019; Weissmann et al., 2010), linked to discharge losses to floodplain processes, infiltration into the loose sediments of the fan, and evapotranspiration (Davidson et al., 2013; Hartley et al., 2010; Horton and DeCelles, 2001; Weissmann et al., 2010). However, some fluvial fan channels have also been shown to widen downstream, possibly due to changes in channel planform or aspect ratio, discharge contribution from groundwater, or discharge capture from adjacent rivers (Chakraborty et al., 2010; Davidson et al., 2013). Fluvial fan channel networks have been studied for qualitative descriptions of channel planform morphology (Davidson et al., 2013; Hartley et al., 2010; Weissmann et al., 2010) and scaling relationships (Davidson et al., 2013; Davidson and Hartley, 2014). Modeling establishes a relationship between the fluvial fan shape and avulsion dynamics, like avulsion trigger period and abandoned channel dynamics (Edmonds et al., 2022; Martin and Edmonds, 2023).

Fluvial fans are distinct landforms from alluvial fans that feature steep gradients (typically 2–12°), have a relatively small radial distance typically less than 10 km, and lack channel networks (Blair and McPherson, 1994; Moscariello, 2018). Although surface channels may occur on alluvial fans, these are transient features formed by surface erosion, and do not construct alluvial fans, which form by a combination of gravitational and sheet flood processes (Blair and McPherson, 1994; Moscariello, 2018). Thus, alluvial fans are not considered here as they are distinct from fluvial fan channel networks that form by river avulsions.

2.3 Morphometric Criteria for Recognition of Delta and Fluvial Fan Channel Networks

Based on the above differences in delta and fluvial fan morphodynamics, we hypothesize that the morphometric differences in their channel networks can be quantified. Based on prior work, we expect river-dominated delta channel networks to display downstream decreasing channel widths and lengths with increasing bifurcation order (Edmonds and Slingerland, 2007; Seybold et al., 2007; Wolinsky et al., 2010), and have an average channel network angle of approximately 72° (Coffey and Shaw, 2017). These metrics should differ in fluvial fans, because the channel networks are built by river avulsions rather than mouth-bar-driven bifurcations. However, delta networks also experience (lobe-scale) avulsions, and we expect some overlap in the network angles. Below, we test these morphometric criteria on 40 river-dominated delta and 40 fluvial fan channel networks (Fig. 3).

3 Dataset and Methods

Although automated channel mapping tools like ChannelExtractor in TopoToolbox (Schwanghart and Kuhn, 2010) and RivaMap (Isikdogan et al., 2017) exist, these methods rely on either terrain-based flow routing or the detection of active surface water, typically based on spectral characteristics, to delineate river channels. However, fluvial fan channel networks are predominantly composed of paleo-channels that lack both clear topographic expression and surface water signatures. Both delta and fluvial fan channels can also be only a few meters wide, often falling below the spatial resolution of commonly available DEMs and remote sensing imagery. In such settings, the coarse resolution and smoothing of subtle terrain in DEMs, especially in low-relief environments, further limit the effectiveness of automated extraction. As a result, we are constrained to manual digitization, as described below.

3.1 Channel Order

To establish channel order in networks, we follow Dong et al. (2016). Their method follows a simple rule: bifurcations produce downstream increasing channel order through channels that branch. To be considered a channel of a higher order, the resultant channels must not merge downstream. When a first-order channel bifurcates, two second-order channels develop downstream of this bifurcation. When these two channels subsequently bifurcate, two new pairs of third-order channels form, and so on (Fig. 4a, b). All channels from the first instance of branching up to and including those that enter a body of water or terminate on land are measured. Identification of bifurcation nodes follows Edmonds et al. (2011), such that the first-order bifurcation for a river channel is the first bifurcation that the channel undergoes (Fig. 4a). Although these methods were developed for deltaic channel networks, here we adapt them for fluvial fan networks (Fig. 4c, d). We do not map or measure channels that loop or rejoin downstream, or channels of non-fluvial origin, such as tidal channels or inlets (Smart and Moruzzi, 1971; Tejedor et al., 2015) that are not connected to the fluvial distributary channels. We also omit local avulsions on fluvial fans, which generate channels that typically merge downfan (Slingerland and Smith, 2004). Paleo-channels on fluvial fans were recorded where possible. Paleo-channels resembled active channels that exhibit little to no discharge when we mapped the chan-

nel networks (Fig. 4c, d). We included paleo-channel measurements in fluvial fans because they are ubiquitous in fluvial fans (Hartley et al., 2010), and many of these channels do carry discharge if reactivated during major flood events.

3.2 Channel Length and Width Measurements

Channel length and width measurements follow Edmonds and Slingerland (2007), where channel length is measured as the distance between two bifurcation nodes in deltas (Fig. 4a). We adopt this methodology also to fluvial fans to measure channel lengths between avulsion nodes (Fig. 4c). The average width of a channel segment is recorded from three separate width measurements: one immediately after a node (w_i), one immediately before the next node (w_f), and one halfway between these two points at the midpoint of the channel segment (w_h) (Fig. 4a, c). Land–water boundaries in both deltas and fluvial fans were identified visually based on color (with water appearing darker and bluer than land), surface texture, and vegetation contrast. In deltas, channel width measurements were recorded based on the width of water present in the channel, which was nearly always delineated by clear vegetation (Fig. 4b). For channels on fluvial fans, including paleo-channels, bankfull widths were measured from clearly identifiable channel banks, vegetation patterns, and subtle depressions, allowing for the mapping of dry or inactive channels (Fig. 4d). These approaches allowed measurement of inactive channels while maintaining a uniform methodology and consistency for all width measurements. The smallest measured channel widths resolvable in the imagery were 2 m for deltas and 1 m for fluvial fans. Width measurements were not performed in locations where a channel has locally split into multiple branches that join downstream.

Given the maximum 0.5 m spatial resolution of the imagery (see Methods Sect. 3.5), measuring channels only a few meters wide carries some uncertainty. Normalization to the first-order channel width helps mitigate this effect and reduce variability across systems. All channel width measurements were normalized using the initial first-order channel width, following the methodology of Edmonds and Slingerland (2007). Consequently, the normalized channel width value for first-order channels is always equal to one. First-order channel lengths were measured between the last occurrence of tributary channels and the first channel splitting node and contain no significant value for our study. Moreover, manual digitization of fluvial fan channels spanning tens of kilometers may introduce minor inconsistencies in channel path representation, particularly for narrow (< 10 m) and highly sinuous channels. All channel length measurements (l) were also normalized using the first-order channel width measurements according to existing methodologies (Edmonds and Slingerland, 2007; Jerolmack, 2009), and this too helped to reduce uncertainties when digitizing channel lengths. As such, the normalized first-order channel length values merely reflect our selected methodologies rather than an attributable morphological characteristic.

3.3 Network Angle Measurements

To quantify network angles, we adopt the methodology of Coffey and Shaw (2017) developed for measuring channel bifurcation angles, which determines the angles of mouth bars formed at the end of an upstream channel. In this methodology, the final channel width directly upstream of a bifurcation (w_f) is set as the length for two limbs of an angle that follows the mouth bar-water contact to measure a bifurcation angle (θ_n) (Coffey and Shaw, 2017) (Fig. 4b). The same methodology is adapted here for fluvial fans (Fig. 4d). In some river deltas, tidal processes cause bifurcation of a channel into three channels instead of two; these are referred to as trifurcations (Leonardi et al., 2013), furcation (Shaw et al., 2018), or polyfurcations (Chamberlain et al., 2018), and a few such measurements are included in the dataset in the very distal portions of deltas where tidal influence is significant. We do not measure angles where channels loop or rejoin downstream of avulsions or bifurcations. In essence, we focus on the morphology of branching channel networks and measure the visible angles between channels or paleo-channels independent of their origin (Fig. 4b, d).

3.4 Global Delta and Fluvial Fan Channel Network Database

To test the applicability of the proposed criteria, we selected 40 river-dominated deltas and 40 fluvial fans (Fig. 3 and the Supplement) to be mapped using composite satellite data (Esri, 2025). These landforms were selected from a diverse range of hydroclimatic, topographic, and basinal conditions from across the world (Fig. 3).

All deltas have been identified as such by prior work (Broaddus et al., 2022; Galloway, 1975; Hartley et al., 2010; Leier et al., 2005; Nienhuis et al., 2015, 2018; Vulis et al., 2023), and they display active discharge based on satellite imagery. Only river-dominated deltas are included in the dataset, because wave-and tide-dominated delta morphology is distinct from that of fluvial fans. The river dominance of deltas and the presence of tide- or wave-influence was determined using the established principles of process-based delta classification (Broaddus et al., 2022; Galloway, 1975; Nienhuis et al., 2015, 2018; Paniagua-Arroyave and Nienhuis 2024; Vulis et al., 2023). However, categorical discrepancies exist between these different classification approaches. To clarify our terminology, we define "dominated" versus "influenced" deltas as follows. Wave-dominated deltas (e.g. São Francisco, Eel) are characterized by strandplains and a complete absence of bifurcations; these deltas are excluded from our study. Wave-influenced deltas still possess morphological features such as strandplains, but exhibit clear, measurable channel bifurcations and are included in our study. Sim-

ilarly, tide-dominated deltas (e.g. Fly, Yangtze) have a limited number of channels that widen substantially seaward, whereas tide-influenced deltas such as the Yukon (Fig. 1c) exhibit channel widening only in the most distal channels (Xu and Plink-Björklund, 2023). In practice, we combine these parameters with established classifications (Broaddus et al., 2022; Galloway, 1975; Nienhuis et al., 2015, 2018; Paniagua-Arroyave and Nienhuis, 2024; Vulis et al., 2023) to categorize the deltas in our study. Please refer to the Supplement for information regarding our classification of each delta. We test the effects of tide- and wave-influence on the morphometric criteria by comparative analyses.

Fluvial fans were located using their apex coordinates from the global fluvial fan database of Hartley et al. (2010). This database also includes data on fluvial fan length, gradient, termination style (axial, contributory, lacustrine, marine, playa, desert/dune, and wetland). Termination styles refer to the environment where the fluvial fan terminates: for instance, a contributory-termination style denotes that the landform channels switch from distributary to contributory at the toe of the fan, while axial fans are classified when the main channel forms a confluence with an axial fluvial system (Hartley et al., 2010). Fluvial fans that enter oceans or lakes were originally distinguished from deltas based on (1) displaying no significant modification of the planform by marine processes, such as wave or tidal influence; or (2) the fluvial fans apex is close to the tidal limit (Hartley et al., 2010). They identified that on relatively high-gradient systems (with slopes above 0.143°) marine reworking is normally restricted to the toe of the fluvial fans and can be easily identified. On relatively low-gradient systems (with slopes below 0.0573°) the influence of marine processes was more difficult to determine, and unless the landform apex was located a significant distance inland (> 200 km) the landform was excluded from their database. We added a visual inspection that the channel network is a paleo-channel network, and we test the robustness of the classification by comparative analyses of fluvial fans with lake and ocean terminations versus terrestrial terminations. To further test the robustness of our methodology, we analyze whether the landform size, gradient, termination style, or wave- and tide-influence in deltas affect the results.

3.5 Mapping with ArcGIS Pro

Delta and fluvial fan channel networks were mapped using ArcGIS Pro software (Version 3.2.1) (Figs. 1, 2, and 4) with the ESRI World Imagery basemap, which provides up to 0.5 m imagery for most of the world (Esri, 2025). This resolution is suitable for mapping very narrow channels only several meters wide. Alternative datasets such as Landsat (30 m resolution) or Sentinel-2 (10 m resolution) are too coarse for this application; however they do contain multispectral bands that could be useful in defining land-water contacts in places where it is ambiguous for wider channels. While ESRI World Imagery is compiled from multiple providers and acquisition times, producing mosaicked tiles, we did not observe noticeable changes in channel appearance across tile boundaries (e.g., abrupt changes in channel width or discharge).

Another limitation of our dataset is uncertainty regarding the timing of satellite image acquisition relative to precipitation events. Precipitation increases discharge, thereby increasing measured channel widths, particularly for fluvial fans in arid environments. Such events can also reactivate partial avulsions and crevasses, which can potentially increase the apparent number of channels. However, none of the selected systems exhibited observable seasonal or large-scale discharge changes across their channel networks attributable to different timings in data collection. Additionally, because this study relies on values normalized to the initial channel width, the effects of seasonal variability on channel width measurements are minimized.

Two feature classes were created: one for deltas and one for fluvial fans. Each delta or fluvial fan landform was then individually mapped as a shapefile layer under the corresponding feature class (the Supplement). The shapefiles for channel networks were created as polyline features, which allow users to manually trace individual river channel segments while automatically recording line lengths. Channel widths and angles were measured using the line and angle measurement tools in ArcGIS Pro. All data were recorded in the attribute table for each landform. These data were organized into Excel documents and subsequently converted to Python- and Pandas-readable CSV files (the Supplement).

3.6 Code and Statistics

Kolmogorov–Smirnov (KS) and Shapiro–Wilk (SW) tests were first applied to determine whether the data are normally distributed. Levene's test was used to test differences in variances of populations that do not exhibit a normal distribution (Trauth, 2006). Independent samples t-test or Welch's t-test were then applied to test for a difference in means for populations with similar and dissimilar variances, respectively, while one-sample t-tests were used to test comparisons of a subgroup against the overall population mean (Trauth, 2006). For this study, a p value less than 0.05 (5 % significance level) suggests that the two population distributions, variances, or means are not similar. Data confidence intervals were calculated according to Mendenhall et al. (2012). Data analysis and visualization were performed using Python. Open-source data visualization libraries Matplotlib (Hunter, 2007), NumPy (Harris et al., 2020), SciPy (Virtanen et al., 2020), and Seaborn (Waskom, 2021) were utilized.

4 Results

4.1 Delta and Fluvial Fan Channel Network Angles

The mean channel network angle (θ_d) in deltas is 74.0° with a 95 % confidence interval of ±1.9° ($n = 527$) (Fig. 5a). The mean channel network angle (θ_f) in fluvial fans is 55.0° ± 2.0° ($n = 520$) (Fig. 5b). The delta and fluvial fan network angle populations are not normally distributed according to both Kolmogorov–Smirnov and Shapiro–Wilk tests, with p values less than 0.05. Levene's test for statistical difference in variances also results in a p value less than 0.05, suggesting population variances are statistically different. A subsequent independent sample t-test suggests the means of delta and fluvial fan angle populations are statistically different, with a p value less than 0.05. All statistical results are recorded in Table S1 in the Supplement.

We also reviewed the mean network angle of each individual delta and fluvial fan ($\theta_{Landform}$) (Fig. 5c, d), and these analyses reveal some overlap. All fluvial fans have mean angle values less than 60°, except for six landforms, or 15 % of fluvial fans in this study. Four of these landforms have mean angles larger than 60° (60.8, 63.2, 67.7, and 67.9°), and two larger than the delta mean of 73.7° (79.6 and 80.1°). All individual deltas have mean network angles larger than 60°, except for one delta (59.3°). There are also three deltas with mean angles around 60° (61.5, 62.4, and 63.3°).

The distribution of delta angles grouped by order (Fig. 6a) yields no strong trends for mean angle in deltas. Seventh and tenth order channels have slightly lower mean angle values at 65 and 67°, but these higher-order groups have low sample sizes ($n = 3$; $n = 8$) (Fig. 6a). The distribution of fluvial fan angles grouped by order does yield a trend: the mean angle for first- through third-order channels (θ_1, θ_2, and θ_3 in Fig. 6b) is between 47–50° and increases to 61–63° for fourth- through eighth-order channels, and to 66° for ninth-order angles ($n = 6$) (θ_4–θ_9 in Fig. 6b). In contrast to the unimodal distribution of delta angles, the distribution of higher-order fluvial fan angles is bimodal, with a dominant peak near 50° and a secondary peak around 80–100° (Fig. 6b).

All deltas in this analysis are river-dominated deltas, however some are tide- or wave-influenced (see Sect. 3.4 and the Supplement). Grouping deltas by process regime shows that the mean network angle for the 19 river-dominated deltas ($\theta_R = 73.6 \pm 2.2°$, $n = 374$), for the 16 tide-influenced deltas ($\theta_t = 75.6 \pm 3.9°$, $n = 139$), and for the 5 wave-influenced deltas ($\theta_w = 67.1 \pm 10.1°$, $n = 14$) (Fig. 7a). The river-dominated and tide-influenced delta angle means are not statistically different from the mean angle for the whole delta population (Table S1). The wave-influenced delta angles were omitted from this statistical analysis due to a small sample size ($n = 14 < 30$).

Many delta angle measurements in this dataset come from Arctic deltas. The comparison between Arctic and non-Arctic deltas shows that Arctic deltas have a larger mean angle ($\theta_A = 76.5 \pm 2.7°$, $n = 263$) than non-Arctic deltas ($\theta_{NA} = 71.4 \pm 2.6°$, $n = 264$) (Fig. 7b). There is a statistically significant difference in means between Arctic and non-Arctic deltas (Table S1). Grouping deltas by termination style (Fig. 7c) shows that lake-terminating deltas have slightly smaller mean angles than those that terminate in oceans ($\theta_L = 72.9 \pm 3.2°$, $n = 160$, versus $\theta_O = 74.4 \pm 2.3°$, $n = 367$), but these differences are not statistically significant compared to the whole delta population (Table S1).

Grouping fluvial fans by their termination style shows some differences (Fig. 7d), where the mean angles vary from a low of $\theta_{axial} = 45.4 \pm 4.2°$ ($n = 57$) for axial-terminating fluvial fans to $\theta_{wetlands} = 61.1 \pm 8.9°$ ($n = 37$) for wetland-terminating fans (Fig. 7d). All fluvial fan termination types, except for axial-terminating fans, exhibit population means that are statistically similar to the overall fluvial fan population (Table S1). However, each termination style is represented by only 4 to 6 landforms, limiting the statistical power of comparisons and generalizations, despite the relatively robust measurement numbers in wetland ($n = 37$), playa ($n = 45$), dunes/desert ($n = 51$), and axial-terminating fans ($n = 57$). There also appears to be some discrepancies in Hartley et al. (2010)'s assignment of termination types, such as referring to playa fans as lacustrine or ocean fans as contributory. We also tested whether landform size (Fig. S1 in the Supplement) and gradient (Fig. S2) affect the channel network angles, and these analyses yield no trends, supporting the robustness of our methodology.

4.2 Channel Lengths and Widths

Normalized channel length and width measurements reveal morphological differences between fluvial fan and delta channels. Both landform types show non-linear decreases in these values with increasing channel order (Fig. 8). Statistical analyses confirm that the overall means for normalized channel length and width differ significantly between fluvial fans and deltas (Table S1). Fluvial fan channels are generally an order of magnitude longer than delta channels, with a mean normalized length of 147.09 compared to 17.18 for deltas (Fig. 8a, c). In contrast, delta channels tend to be slightly wider, with a mean normalized width of 0.40 compared to 0.26 for fluvial fans (Fig. 8b, d).

Comparing the normalized dimensions by channel order (Fig. 9) reveals additional trends. The normalized channel lengths of lower-order fluvial fan channels (orders 1–5) are significantly longer, and the channel shortening rate is higher compared to deltas (Fig. 9a). The normalized lengths become very similar in orders 7–8, then diverge again for the higher orders where the fluvial fan channel lengths are somewhat longer, but the channel shortening rates are higher in deltas. Normalized channel widths show significant differences for orders 2–8, but not for 9–11. Only a few landforms have channels with orders exceeding 9. Fluvial fan narrowing rates are very high from orders 1 and 2, and very low

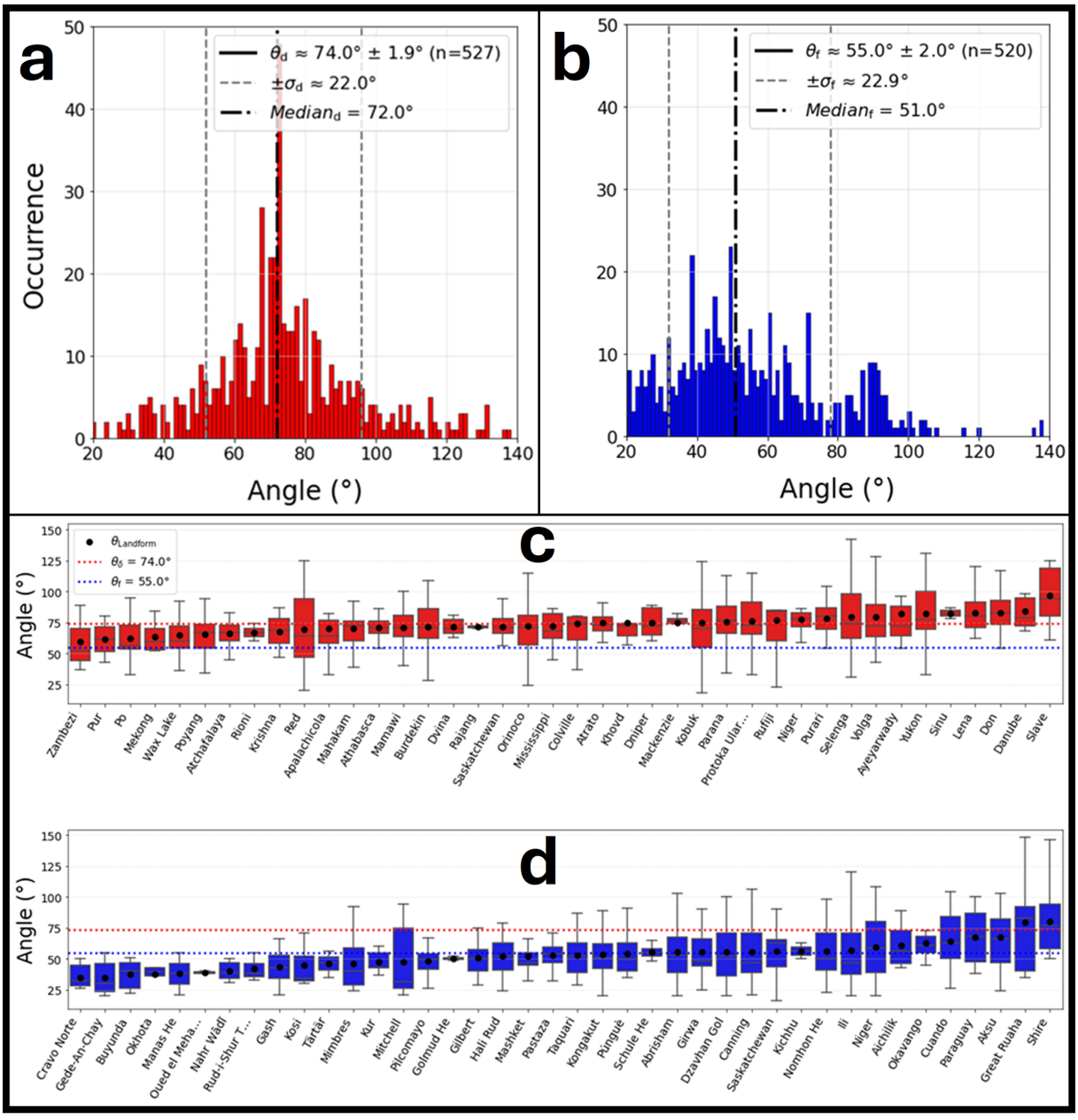

Figure 5. Histograms depicting distributions of **(a)** delta channel network angles with mean angle (θ_d), its standard deviation (σ_d) and median, and **(b)** fluvial fan channel network angles with mean fan angle (θ_f), its standard deviation (σ_f)and median. Box-and-whisker plots with the mean angle for each delta **(c)** and fluvial fan **(d)** landform ($\theta_{Landform}$).

in orders 7–10 (Fig. 9b). The narrowing rates are more uniform in deltas. When comparing individual deltas by process regime, both tide- and wave-influenced deltas have significantly higher mean normalized channel widths relative to the overall delta population (Fig. S3 and Table S1).

Comparison by fluvial fan termination styles shows that axial- and playa-terminating fans exhibit longer mean normalized channel lengths compared to the whole fluvial fan population, whereas dunes/desert-, marine-, and wetland-terminating fans have shorter mean lengths (Fig. S3 and Table S1). Contributory- and lake-terminating fans do not differ significantly from the overall mean. Regarding normalized channel widths, axial- and marine-terminating fans have wider channels, while dunes/desert-terminating fans are narrower. Normalized width values for contributory-, lake-, playa-, and wetland-terminating fan channels show no difference from the overall population mean (Fig. S3 and Table S1). Statistical analyses of channel length and width were not conducted for different fluvial fan termination styles due to insufficient sample sizes ($n < 30$) in most categories.

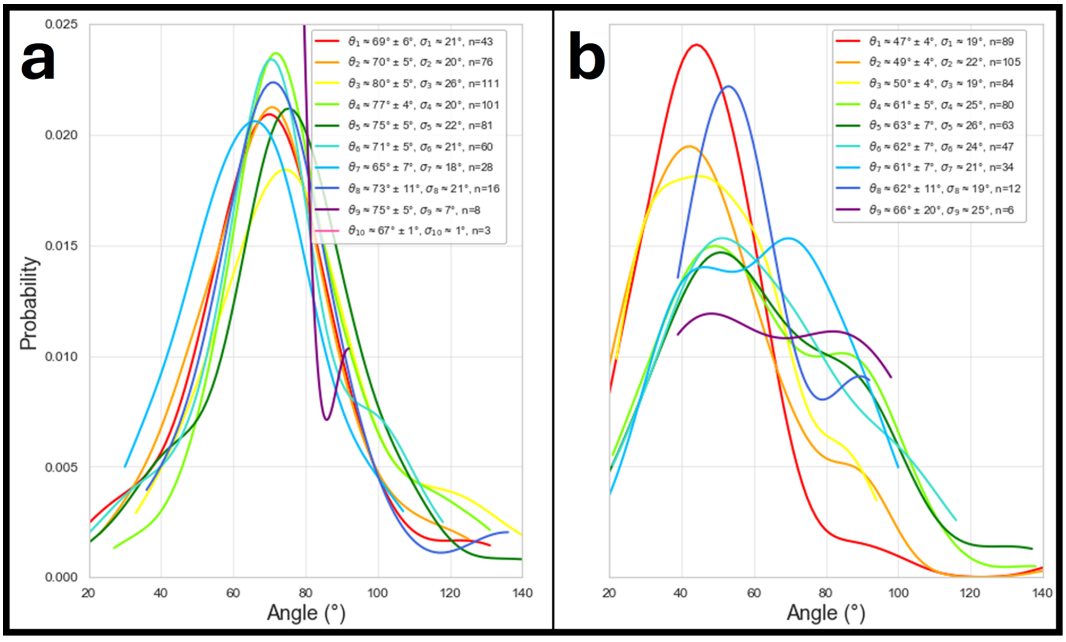

Figure 6. Distribution of **(a)** delta, and **(b)** fluvial fan network angles grouped by order (θ_n) with the 95 % confidence interval. (σ_n) = denotes standard deviation. n denotes sample size.

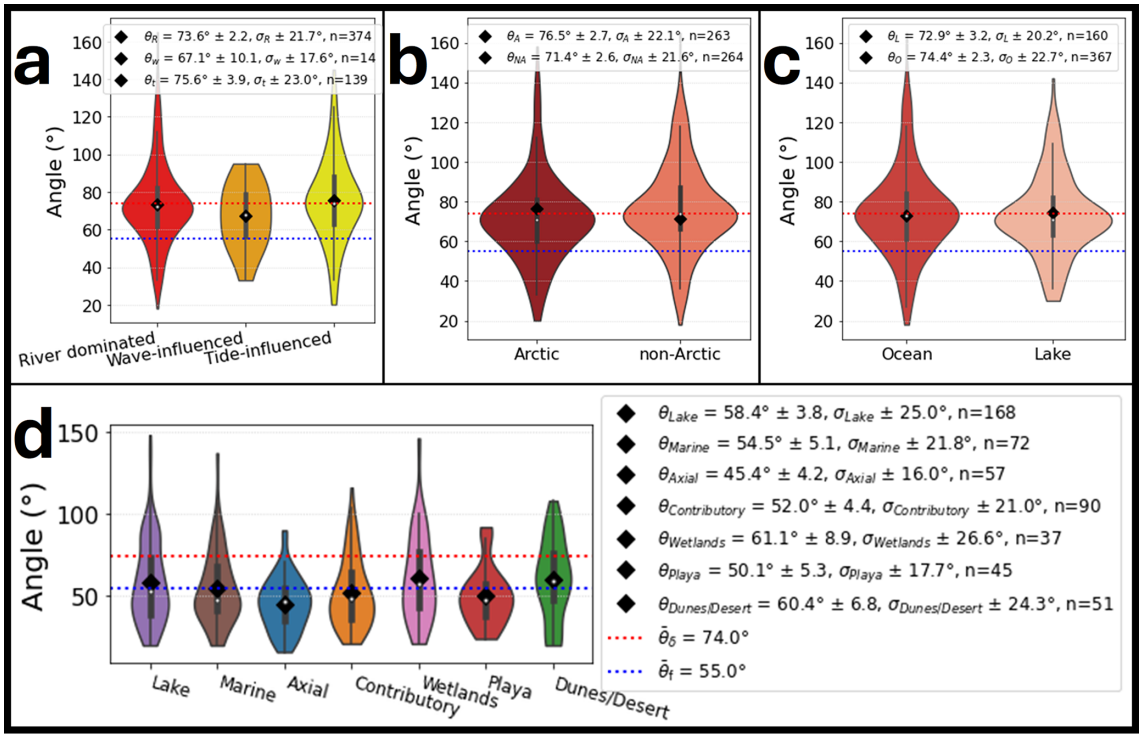

Figure 7. Violin plots depicting network angle distributions by **(a)** delta process regime: river dominated (θ_R), wave-influenced (θ_w), and tide-influenced (θ_t), **(b)** deltas in non-Arctic (θ_{NA}) and Arctic (θ_A) climates, **(c)** ocean terminating deltas (θ_O) and lake terminating deltas (θ_L), and **(d)** fluvial fan termination styles. All mean angle values have a corresponding 95 % confidence intervals, standard deviation (σ), and sample count (n).

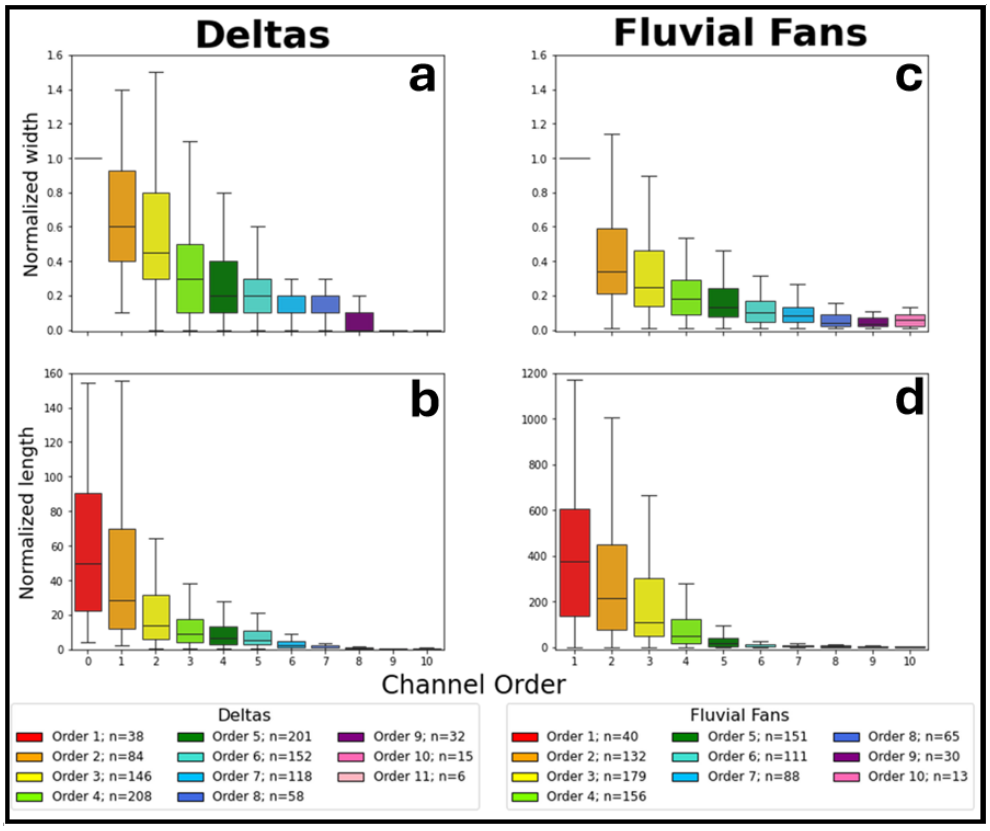

Figure 8. Box and whisker plots illustrating normalized delta channel widths **(a)** and lengths **(b)**, and normalized fluvial fan channel widths **(c)** and lengths **(d)**, plotted by channel order. Note the significant difference in normalized channel length scales for panels **(b)** and **(d)**.

5 Discussion

5.1 Effectiveness of Morphometric Criteria in Distinguishing Deltas and Fluvial Fans

The mean channel network angles are distinctly different in deltas and fluvial fans by 20°, and this statistically significant difference is a useful criterion in distinguishing these two landform types. While some overlaps exist at the landform level, these cases are relatively limited, where 15 % of fluvial fans in this dataset have a mean angle larger than 60° (Fig. 5d) and 10 % of deltas have a mean angle less than 64° (Fig. 5c). These findings support the utility of mean branching angles as a distinguishing metric between deltas and fluvial fans. However, some degree of uncertainty remains, and additional criteria are necessary for more robust distinction.

An additional criterion is the distribution of mean angles by channel order, where fluvial fans have increased mean angles and a bimodal distribution in orders 4–8 (Fig. 6). Other supportive criteria may be the differences in values and distributions of the normalized channel lengths and widths (Figs. 8 and 9), but the low sample numbers do not allow us to test these criteria by individual landforms. A useful criterion would be to link channel narrowing with the bifurcation and avulsion nodes. In deltas, the downstream channel narrowing occurs in a stepwise manner at the mouth-bar-driven bifurcation nodes, whereas in fluvial fans this decrease should be gradual and not linked to the node positions where full avulsions occur. Our data were collected in a manner that does not permit these analyses.

A potential source of overlap in the delta and fluvial fan channel network mean angles is that not all measured angles in deltas are mouth-bar-driven bifurcation angles, as deltas also experience avulsions (e.g., Fig. 1h). A closer inspection of the four deltas with low mean network angles reveals that each contains very few measurements ($n = 3$, $n = 4$, $n = 6$, $n = 7$). In these cases, the limited sample size allows the rarer avulsion angles to affect the mean values more strongly. Also, fluvial fans that terminate in a lake or ocean may have terminal channels that form due to mouth bar deposition and channel bifurcation. However, we do not believe these instances affect our results, since we do not see that lake- or marine-terminating fans exhibit higher mean angles (Fig. 7d).

Examining fluvial fans with high mean angles shows that these are low-gradient wetland fans, where the avulsion angles tend to be wider as a function of avulsion mechanisms

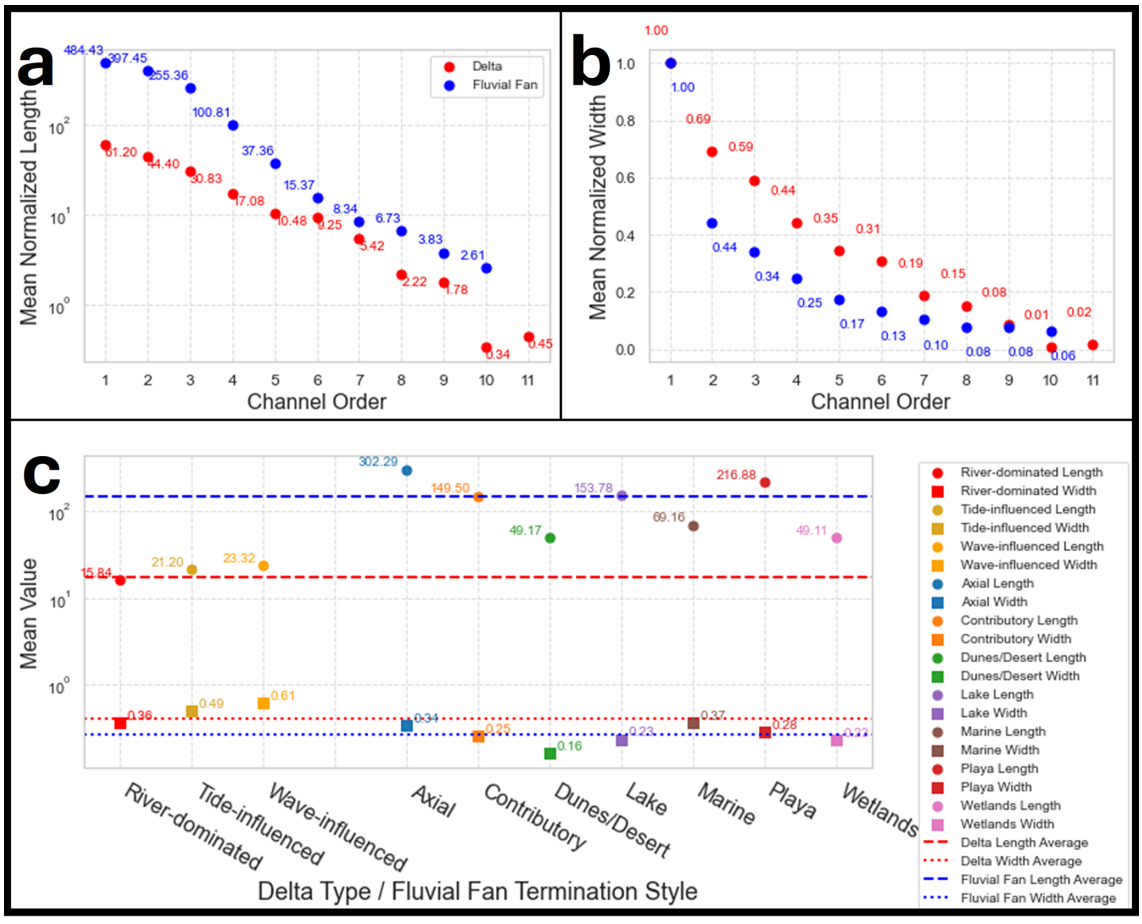

Figure 9. Mean normalized delta and fluvial fan channel **(a)** length and **(b)** width values by order. **(c)** Mean channel length and width values for different types of deltas and fluvial fan termination styles.

(see Discussion below). However, they may also suggest methodological limitations. While the local avulsion angles in low-gradient wetland fans are wide (using the final channel width directly upstream of a branching node (w_f) as the length for two limbs of an angle; Fig. 4b), angles between the longer channel reaches are considerably narrower (Fig. S4). This channel reach angle discrepancy is consistent with similar channel reach angle measurements from Coffey and Shaw (2017). We plan to further develop angle measurement methods to capture both the local and the reach-scale angles in future work. It is also important to discuss the limitations of the applied methodologies in the context of the results. Our channel network methodologies are designed for delta channel networks, and exclude channels that merge downstream, which can exclude many potential measurements from fluvial fans in situations where their channels merge downfan.

In summary, this initial attempt to distinguish deltas and fluvial fans demonstrates that quantifying channel network angles, and trends in normalized channel widths and lengths provide efficient criteria. However, we also show that sample sizes are important for accurate recognition of landforms, and collecting a sufficient number of angle measurements ($n \gtrapprox 10$) can help account for the infrequent avulsion in deltas or bifurcation in fluvial fans. While each metric is informative on its own, the combination of branching angles, branching angle trends, and normalized channel lengths provides the clearest distinction between deltas and fluvial fans.

5.2 Processes that determine delta and fluvial fan channel network angles

While the 72° mean mouth-bar-driven bifurcation angle is linked to flow patterns at channel tips well-explained by diffusive processes (Coffey and Shaw, 2017), there is currently no established explanation for the approximately 55° mean network angle in fluvial fans. In deltas, mouth-bar-driven bifurcation is the product of sedimentation from turbulent jets that form at the mouths of rivers entering basins (Bates, 1953; Coffey and Shaw, 2017; Edmonds and Slingerland, 2007; Fagherazzi et al., 2015; Jerolmack and Swenson, 2007; Wright, 1977). Once a mouth bar is formed, the flow through the distributary channel bifurcations can be modeled as diffu-

sive flow (Coffey and Shaw, 2017), and the resulting critical angle of 72° represents a stable morphology for the bifurcation as it grows in a diffusive groundwater field (Devauchelle et al., 2012; Ke et al., 2019). The slightly larger network angles in Arctic deltas may reflect environmental influences such as ice cover, permafrost, or limitations on overbank flow (Lauzon et al., 2019; Piliouras et al., 2021; Walker, 1998).

River avulsions are set up by channel superelevation (Mohrig et al., 2000), or when the slope down the flanks of the channel provides a steeper descent than the existing river channel (Slingerland and Smith, 1998; Törnqvist and Bridge, 2002). Avulsions result from channel bed aggradation that reduces the channel capacity (Bryant et al., 1995). Once an avulsion is triggered and full or partial river flow exits the channel, a new channel is generated by surface runoff erosion. Thus, the prevailing topographic gradient would tend to keep the nearby flows more focused in a slope-parallel direction, resulting in narrower network angles compared to mouth-bar-driven bifurcations (Fig. 5b).

The contrast between diffusion-dominated and surface runoff erosion-dominated processes in shaping delta versus fluvial fan channel network topology is further supported by tributary channel network analyses that originally defined the critical angle of 72° (Devauchelle et al., 2012). Tributary channel network analyses show that the mean tributary angle of 72° only occurs in humid catchments with high groundwater recharge, where tributary networks are shaped by groundwater diffusion (Seybold et al., 2017). In contrast, the mean tributary network angle is 45° in arid landscapes where surface runoff dominates (Seybold et al., 2017), or is even lower in the driest catchments (Seybold et al., 2018).

Fluvial fan gradient decreases progressively downstream (e.g. Chakraborty et al., 2010), such that higher gradients near the fan apex likely generate more acute angles, whereas the very low gradients near the toe of the fan would allow for wider angles. This trend likely explains the downstream increase in fluvial fan network angles and the emergence of the second, wider peak in higher order channels (Fig. 6b). Furthermore, avulsion mechanisms have been shown to change from channel superelevation in upstream river reaches, where river gradients are steeper, to gradient advantage in downstream low-gradient reaches (Gearon et al., 2024). In these low-gradient zones, crevassing processes can produce high-angle deviations with the angle values around 90° (Rahman et al., 2022). Avulsion angles above 100° have been measured in meandering rivers on low-gradient floodplains with vegetation (see Rahman et al., 2022). These effects may be important controls in the fluvial fan channel networks in low-gradient vegetated wetlands. Reitz and Jerolmack (2012) show that abandoned paleo-channel reoccupation may control new avulsion positions, and paleo-channel density is highest in the narrower fan apex. Avulsion angles may also change over time due to evolving channel width ratios (Morais and Montanher, 2022), or may be affected by a critical angle or bend curvature (Yang, 2020). Future work targeting how avulsion morphology evolves downfan would provide important insight into the mechanisms driving the observed increase in angles downstream.

We thus conclude that the distinction between deltaic and fluvial fan channel network angles arises from the dominant formative processes: diffusive flow in deltas versus surface runoff erosion in fluvial fans. Furthermore, in fluvial fans, network angles appear to be negatively correlated with surface gradients, with lower gradients allowing for wider avulsion angles.

5.3 Ancient deltas and fluvial fans

Our proposed methodology could also be used to distinguish ancient fluvial fans and deltas, for instance in seismic datasets, where only delta channel network angles have been quantified before (Mahon et al., 2024). Our results confirm the prior modern data (Chakraborty et al., 2010) and recent modeling outcomes (Martin and Edmonds, 2023), and help to eliminate a discrepancy in plan-view versus cross-sectional fluvial fan facies models (Plink-Björklund, 2021). Namely, earlier work suggested processes similar to mouth-bar-driven bifurcations as a key mechanism driving fluvial fan formation (Friend, 1978; Kelly and Olsen, 1993; Weissmann et al., 2010), probably due to downstream channel narrowing. However, this hypothesis contradicts the stratigraphic data that indicate that proximal fans consist of amalgamated channel deposits (Chakraborty et al., 2010; Kelly and Olsen, 1993; Nichols and Fisher, 2007; Singh et al., 1993; Weissmann et al., 2013) – a pattern consistent with frequent avulsions (Chakraborty et al., 2010; Singh et al., 1993).

5.4 Sensitivity of Deltas and Fluvial Fans to Global Change

Deltas and fluvial fans differ significantly in their vulnerability to natural hazards and in their responses to global change. Deltas are highly vulnerable to coastal hazards and sea-level rise (Giosan et al., 2014; Syvitski et al., 2009). Rising sea-levels will not only inundate deltaic distributary networks, but also cause a landward migration of the avulsion node corresponding with the landward shift of the backwater zone (Brooke et al., 2022; Chatanantavet et al., 2012; Ganti et al., 2014). This process reduces sediment delivery to shorelines, accelerating the effects of sea-level rise. However, changes in land use and changing precipitation patterns which increase sediment supply could complicate the picture by shifting delta avulsion sites seaward (Brooke et al., 2022). In contrast, fluvial fans are controlled by upstream morphodynamics, where the fan location (apex) is pinned by a steep topographic break (Brooke et al., 2022; Ganti et al., 2014; Martin and Edmonds, 2023). For coastal fans, sea-level rise and coastal erosion would affect the fan toes, however the avulsion node at the fan apex and sediment deposition across

most of the fan surface would not be affected, making fluvial fans significantly less vulnerable to sea-level rise.

Both deltas and fluvial fans are affected by reduced sediment supply due to river damming and artificial levees (Blum and Roberts, 2009; Giosan et al., 2014; Nienhuis et al., 2020; Paola et al., 2011; Syvitski et al., 2009). However, fluvial fans are highly sensitive to the water and sediment supply changes, such as changes in precipitation patterns (Assine et al., 2014; Hansford and Plink-Björklund, 2020; Leier et al., 2005). Increases in extreme precipitation cause a significant increase in avulsion frequency and crevassing splay formation (Morón et al., 2017), because large fluctuations in river discharge, such as during extreme precipitation events, are avulsion-triggering events (Jones and Schumm, 1999). Indeed, fluvial fans have been shown to be highly sensitive to such changes, where fluvial fan activation and deactivation cycles have been linked to millennial-scale changes in monsoon intensity or precipitation patterns (Assine et al., 2014; Fontana et al., 2014; Latrubesse et al., 2012).

6 Conclusions

This study demonstrates that river-dominated delta and fluvial fan channel networks can be distinguished using quantitative morphometric criteria derived from their channel network topology. Deltaic networks are primarily shaped by mouth-bar-driven bifurcation processes, resulting in mean bifurcation angles of approximately 74°, consistent with diffusion-dominated growth. In contrast, fluvial fan topology is shaped by channel avulsions, producing narrower mean network angles near 55°, indicative of surface runoff processes. Fluvial fan network angles tend to widen downstream, likely due to decreasing gradients and avulsion style shifts, while delta angles remain relatively consistent, reflecting persistent mouth-bar-driven bifurcation processes. Both channel networks display downstream reductions in channel length and width with increasing channel order, but the fluvial fan networks are characterized by significantly longer and somewhat narrower channels when normalized.

These differences not only support the use of network morphology as a diagnostic tool for identifying ancient fluvial fans and deltas in the stratigraphic record or other planetary bodies but also provide insights into their differing sensitivities to environmental change.

Code availability. The Python code used for data analysis and figure generation was created and run in Jupyter Notebook version 6.4.8 (Anaconda distribution). The code is stored in the data repository https://github.com/lukegezovich/Delta-and-Fluvial-Fan-Networks (last access: 11 December 2025).

Data availability. Morphological data collected in this study are available at https://github.com/lukegezovich/Delta-and-Fluvial-Fan-Networks (last access: 11 December 2025).

Supplement. The supplement related to this article is available online at https://doi.org/10.5194/esurf-14-211-2026-supplement.

Author contributions. LG was responsible for the investigation and data curation, development of methodology, formal analysis and visualization, and writing the original draft of the manuscript. PPB initiated the project, co-developed the initial methodology, and co-wrote the manuscript. JH co-developed the initial methodology and perform initial mapping and analyses of a small number of systems.

Competing interests. The contact author has declared that none of the authors has any competing interests.

Disclaimer. Publisher's note: Copernicus Publications remains neutral with regard to jurisdictional claims made in the text, published maps, institutional affiliations, or any other geographical representation in this paper. While Copernicus Publications makes every effort to include appropriate place names, the final responsibility lies with the authors. Views expressed in the text are those of the authors and do not necessarily reflect the views of the publisher.

Acknowledgements. We thank Kamini Singha, Lesli Wood, and Wendy Zhou for their constructive feedback that helped improve earlier versions of this manuscript. We also thank John Shaw, Ellen Chamberlin, Anastasia Piliouras, and an anonymous reviewer for their helpful comments on the present versions of the manuscript.

Financial support. This work has been supported by the American Association of Petroleum Geologists (AAPG) Foundation John & Erika Lockridge Grant, the American Institute of Professional Geologists (AIPG) William J. Siok Graduate Scholarship, the Colorado Scientific Society (CSS), the Rocky Mountain Association of Geologists (RMAG), and the Society for Sediment Geology (SEPM).

Review statement. This paper was edited by Anastasia Piliouras and reviewed by John Shaw, Ellen Chamberlin, and one anonymous referee.

References

Allen, P. A.: Time scales of tectonic landscapes and their sediment routing systems, SP, 296, 7–28, https://doi.org/10.1144/SP296.2, 2008.

Assine, M. L.: River avulsions on the Taquari megafan, Pantanal wetland, Brazil, Geomorphology, 70, 357–371, https://doi.org/10.1016/j.geomorph.2005.02.013, 2005.

Assine, M. L., Corradini, F. A., Pupim, F. D. N., and McGlue, M. M.: Channel arrangements and depositional styles in the São Lourenço fluvial megafan, Brazilian Pantanal wetland, Sediment. Geol., 301, 172–184, https://doi.org/10.1016/j.sedgeo.2013.11.007, 2014.

Axelsson, V.: The Laitaure Delta: A Study of Deltaic Morphology and Processes, Geogr. Ann. A, 49, 1–127, https://doi.org/10.2307/520865, 1967.

Bates, C. C.: Rational Theory of Delta Formation, AAPG Bulletin, 37, 2119–2162, https://doi.org/10.1306/5CEADD76-16BB-11D7-8645000102C1865D, 1953.

Bentley, S. J., Blum, M. D., Maloney, J., Pond, L., and Paulsell, R.: The Mississippi River source-to-sink system: Perspectives on tectonic, climatic, and anthropogenic influences, Miocene to Anthropocene, Earth-Sci. Rev., 153, 139–174, https://doi.org/10.1016/j.earscirev.2015.11.001, 2016.

Blair, T. C. and McPherson, J. G.: Alluvial Fans and their Natural Distinction from Rivers Based on Morphology, Hydraulic Processes, Sedimentary Processes, and Facies Assemblages, SEPM J. Sediment. Res., 64A, https://doi.org/10.1306/D4267DDE-2B26-11D7-8648000102C1865D, 1994.

Blum, M. D. and Roberts, H. H.: Drowning of the Mississippi Delta due to insufficient sediment supply and global sea-level rise, Nat. Geosci., 2, 488–491, https://doi.org/10.1038/ngeo553, 2009.

Bramble, M. S., Goudge, T. A., Milliken, R. E., and Mustard, J. F.: Testing the deltaic origin of fan deposits at Bradbury Crater, Mars, Icarus, 319, 363–366, https://doi.org/10.1016/j.icarus.2018.09.024, 2019.

Broaddus, C. M., Vulis, L. M., Nienhuis, J. H., Tejedor, A., Brown, J., Foufoula-Georgiou, E., and Edmonds, D. A.: First-Order River Delta Morphology Is Explained by the Sediment Flux Balance From Rivers, Waves, and Tides, Geophys. Res. Lett., 49, e2022GL100355, https://doi.org/10.1029/2022GL100355, 2022.

Brooke, S., Chadwick, A. J., Silvestre, J., Lamb, M. P., Edmonds, D. A., and Ganti, V.: Where rivers jump course, Science, 376, 987–990, https://doi.org/10.1126/science.abm1215, 2022.

Bryant, M., Falk, P., and Paola, C.: Experimental study of avulsion frequency and rate of deposition, Geology, 23, 365–368, https://doi.org/10.1130/0091-7613(1995)023<0365:ESOAFA>2.3.CO;2, 1995.

Chakraborty, T., Kar, R., Ghosh, P., and Basu, S.: Kosi megafan: Historical records, geomorphology and the recent avulsion of the Kosi River, Quatern. Int., 227, 143–160, https://doi.org/10.1016/j.quaint.2009.12.002, 2010.

Chamberlain, E. L., Törnqvist, T. E., Shen, Z., Mauz, B., and Wallinga, J.: Anatomy of Mississippi Delta growth and its implications for coastal restoration, Sci. Adv., 4, eaar4740, https://doi.org/10.1126/sciadv.aar4740, 2018.

Chatanantavet, P. and Lamb, M. P.: Sediment transport and topographic evolution of a coupled river and river plume system: An experimental and numerical study, J. Geophys. Res.-Earth, 119, 1263–1282, https://doi.org/10.1002/2013JF002810, 2014.

Chatanantavet, P., Lamb, M. P., and Nittrouer, J. A.: Backwater controls of avulsion location on deltas, Geophys. Res. Lett., 39, 2011GL050197, https://doi.org/10.1029/2011GL050197, 2012.

Chen, C., Tian, B., Schwarz, C., Zhang, C., Guo, L., Xu, F., Zhou, Y., and He, Q.: Quantifying delta channel network changes with Landsat time-series data, J. Hydrol., 600, 126688, https://doi.org/10.1016/j.jhydrol.2021.126688, 2021.

Coffey, T. S. and Shaw, J. B.: Congruent Bifurcation Angles in River Delta and Tributary Channel Networks, Geophys. Res. Lett., 44, 11427–11436, https://doi.org/10.1002/2017GL074873, 2017.

Davidson, S. K. and Hartley, A. J.: A Quantitative Approach To Linking Drainage Area and Distributive-Fluvial-System Area In Modern and Ancient Endorheic Basins, J. Sediment. Res., 84, 1005–1020, https://doi.org/10.2110/jsr.2014.79, 2014.

Davidson, S. K., Hartley, A. J., Weissmann, G. S., Nichols, G. J., and Scuderi, L. A.: Geomorphic elements on modern distributive fluvial systems, Geomorphology, 180–181, 82–95, https://doi.org/10.1016/j.geomorph.2012.09.008, 2013.

De Toffoli, B., Plesa, A.-C., Hauber, E., and Breuer, D.: Delta Deposits on Mars: A Global Perspective, Geophys. Res. Lett., 48, e2021GL094271, https://doi.org/10.1029/2021GL094271, 2021.

Devauchelle, O., Petroff, A. P., Seybold, H. F., and Rothman, D. H.: Ramification of stream networks, P. Natl. Acad. Sci. USA, 109, 20832–20836, https://doi.org/10.1073/pnas.1215218109, 2012.

Di Achille, G. and Hynek, B. M.: Ancient ocean on Mars supported by global distribution of deltas and valleys, Nat. Geosci., 3, 459–463, https://doi.org/10.1038/ngeo891, 2010.

Dong, T. Y., Nittrouer, J. A., Il'icheva, E., Pavlov, M., McElroy, B., Czapiga, M. J., Ma, H., and Parker, G.: Controls on gravel termination in seven distributary channels of the Selenga River Delta, Baikal Rift basin, Russia, Geol. Soc. Am. Bull., 128, 1297–1312, https://doi.org/10.1130/B31427.1, 2016.

Donselaar, M. E., Cuevas Gozalo, M. C., and Moyano, S.: Avulsion processes at the terminus of low-gradient semi-arid fluvial systems: Lessons from the Río Colorado, Altiplano endorheic basin, Bolivia, Sediment. Geol., 283, 1–14, https://doi.org/10.1016/j.sedgeo.2012.10.007, 2013.

Edmonds, D. A. and Slingerland, R. L.: Mechanics of river mouth bar formation: Implications for the morphodynamics of delta distributary networks, J. Geophys. Res., 112, 2006JF000574, https://doi.org/10.1029/2006JF000574, 2007.

Edmonds, D. A., Paola, C., Hoyal, D. C. J. D., and Sheets, B. A.: Quantitative metrics that describe river deltas and their channel networks, J. Geophys. Res., 116, F04022, https://doi.org/10.1029/2010JF001955, 2011.

Edmonds, D. A., Martin, H. K., Valenza, J. M., Henson, R., Weissmann, G. S., Miltenberger, K., Mans, W., Moore, J. R., Slingerland, R. L., Gibling, M. R., Bryk, A. B., and Hajek, E. A.: Rivers in reverse: Upstream-migrating dechannelization and flooding cause avulsions on fluvial fans, Geology, 50, 37–41, https://doi.org/10.1130/G49318.1, 2022.

Esri: World Imagery, Esri, Maxar, Redlands, CA, https://www.arcgis.com/home/item.html?id=10df2279f9684e4a9f6a7f08febac2a9 (last access: September 2025), 2025.

Fagherazzi, S.: Self-organization of tidal deltas, P. Natl. Acad. Sci. USA, 105, 18692–18695, https://doi.org/10.1073/pnas.0806668105, 2008.

Fagherazzi, S., Edmonds, D. A., Nardin, W., Leonardi, N., Canestrelli, A., Falcini, F., Jerolmack, D. J., Mariotti, G., Rowland, J. C., and Slingerland, R. L.: Dynamics of river mouth deposits, Rev. Geophys., 53, 642–672, https://doi.org/10.1002/2014RG000451, 2015.

Farley, K. A., Williford, K. H., Stack, K. M., Bhartia, R., Chen, A., De La Torre, M., Hand, K., Goreva, Y., Herd, C. D. K., Hueso, R., Liu, Y., Maki, J. N., Martinez, G., Moeller, R. C., Nelessen, A., Newman, C. E., Nunes, D., Ponce, A., Spanovich, N., Willis, P. A., Beegle, L. W., Bell, J. F., Brown, A. J., Hamran, S.-E., Hurowitz, J. A., Maurice, S., Paige, D. A., Rodriguez-Manfredi, J. A., Schulte, M., and Wiens, R. C.: Mars 2020 Mission Overview, Space Sci. Rev., 216, 142, https://doi.org/10.1007/s11214-020-00762-y, 2020.

Federici, B. and Paola, C.: Dynamics of channel bifurcations in noncohesive sediments, Water Resour. Res., 39, 1162, https://doi.org/10.1029/2002WR001434, 2003.

Fielding, C. R., Ashworth, P. J., Best, J. L., Prokocki, E. W., and Smith, G. H. S.: Tributary, distributary and other fluvial patterns: What really represents the norm in the continental rock record?, Sediment. Geol., 261–262, 15–32, https://doi.org/10.1016/j.sedgeo.2012.03.004, 2012.

Fontana, A., Mozzi, P., and Marchetti, M.: Alluvial fans and megafans along the southern side of the Alps, Sediment. Geol., 301, 150–171, https://doi.org/10.1016/j.sedgeo.2013.09.003, 2014.

Friend, P. F.: Distinctive Features of Some Ancient River Systems, in: Fluvial Sedimentology, edited by: Miall, A. D., Canadian Society of Petroleum Geologists, Memoir 5, 531–542, ISBN 978-0920230039, 1978.

Galloway, E.: Process Framework for Describing the Morphologic and Stratigraphic Evolution of Deltaic Depositional Systems, Deltas: Models for Exploration, 1975, 87–98, 1975.

Ganti, V., Chu, Z., Lamb, M. P., Nittrouer, J. A., and Parker, G.: Testing morphodynamic controls on the location and frequency of river avulsions on fans versus deltas: Huanghe (Yellow River), China, Geophys. Res. Lett., 41, 7882–7890, https://doi.org/10.1002/2014GL061918, 2014.

Gearon, J. H., Martin, H. K., DeLisle, C., Barefoot, E. A., Mohrig, D., Paola, C., and Edmonds, D. A.: Rules of river avulsion change downstream, Nature, 634, 91–95, https://doi.org/10.1038/s41586-024-07964-2, 2024.

Geleynse, N., Storms, J. E. A., Walstra, D.-J. R., Jagers, H. R. A., Wang, Z. B., and Stive, M. J. F.: Controls on river delta formation; insights from numerical modelling, Earth Planet. Sc. Lett., 302, 217–226, https://doi.org/10.1016/j.epsl.2010.12.013, 2011.

Giosan, L., Syvitski, J., Constantinescu, S., and Day, J.: Climate change: Protect the world's deltas, Nature, 516, 31–33, https://doi.org/10.1038/516031a, 2014.

Hansford, M. R. and Plink-Björklund, P.: River discharge variability as the link between climate and fluvial fan formation, Geology, 48, 952–956, https://doi.org/10.1130/G47471.1, 2020.

Hariharan, J., Piliouras, A., Schwenk, J., and Passalacqua, P.: Width-Based Discharge Partitioning in Distributary Networks: How Right We Are, Geophys. Res. Lett., 49, e2022GL097897,https://doi.org/10.1029/2022GL097897, 2022.

Harris, C. R., Millman, K. J., van der Walt, S. J., Gommers, R., Virtanen, P., Cournapeau, D., Wieser, E., Taylor, J., Berg, S., Smith, N. J., Kern, R., Picus, M., Hoyer, S., van Kerkwijk, M. H., Brett, M., Haldane, A., del Río, J. F., Wiebe, M., Peterson, P., Gérard-Marchant, P., Sheppard, K., Reddy, T., Weckesser, W., Abbasi, H., Gohlke, C., and Oliphant, T. E.: Array programming with NumPy, Nature, 585, 357–362, https://doi.org/10.1038/s41586-020-2649-2, 2020.

Hartley, A. J., Weissmann, G. S., Nichols, G. J., and Warwick, G. L.: Large Distributive Fluvial Systems: Characteristics, Distribution, and Controls on Development, J. Sediment. Res., 80, 167–183, https://doi.org/10.2110/jsr.2010.016, 2010.

Horton, B. K. and DeCelles, P. G.: Modern and ancient Fluvial megafans in the foreland basin system of the central Andes, southern Bolivia: implications for drainage network evolution in fold-thrust belts, Basin Research 13, 43–63., https://doi.org/10.1046/j.1365-2117.2001.00137.x, 2001.

Hunter, J. D.: Matplotlib: A 2D Graphics Environment, Comput. Sci. Eng., 9, 90–95, https://doi.org/10.1109/MCSE.2007.55, 2007.

Isikdogan, F., Bovik, A., and Passalacqua, P.: RivaMap: An automated river analysis and mapping engine, Remote Sens. Environ., 202, 88–97, https://doi.org/10.1016/j.rse.2017.03.044, 2017.

Jerolmack, D. J.: Conceptual framework for assessing the response of delta channel networks to Holocene sea level rise, Quaternary Sci. Rev., 28, 1786–1800, https://doi.org/10.1016/j.quascirev.2009.02.015, 2009.

Jerolmack, D. J. and Swenson, J. B.: Scaling relationships and evolution of distributary networks on wave-influenced deltas, Geophys. Res. Lett., 34, 2007GL031823, https://doi.org/10.1029/2007GL031823, 2007.

Jones, L. S. and Schumm, S. A.: Causes of Avulsion: An Overview, in: Fluvial Sedimentology VI, edited by: Smith, N. D. and Rogers, J., Wiley, 169–178, https://doi.org/10.1002/9781444304213.ch13, 1999.

Ke, W., Shaw, J. B., Mahon, R. C., and Cathcart, C. A.: Distributary Channel Networks as Moving Boundaries: Causes and Morphodynamic Effects, J. Geophys. Res.-Earth, 124, 1878–1898, https://doi.org/10.1029/2019JF005084, 2019.

Kelly, S. B. and Olsen, H.: Terminal fans a review with reference to Devonian examples, Sediment. Geol., 85, 339–374, 1993.

Latrubesse, E. M., Stevaux, J. C., Cremon, E. H., May, J.-H., Tatumi, S. H., Hurtado, M. A., Bezada, M., and Argollo, J. B.: Late Quaternary megafans, fans and fluvio-aeolian interactions in the Bolivian Chaco, Tropical South America, Palaeogeogr. Palaeoclimatol. Palaeoecol., 356–357, 75–88, https://doi.org/10.1016/j.palaeo.2012.04.003, 2012.

Lauzon, R., Piliouras, A., and Rowland, J. C.: Ice and Permafrost Effects on Delta Morphology and Channel Dynamics, Geophys. Res. Lett., 46, 6574–6582, https://doi.org/10.1029/2019GL082792, 2019.

Leier, A. L., DeCelles, P. G., and Pelletier, J. D.: Mountains, monsoons, and megafans, Geology, 33, 289–292, https://doi.org/10.1130/G21228.1, 2005.

Leonardi, N., Canestrelli, A., Sun, T., and Fagherazzi, S.: Effect of tides on mouth bar morphology and hydrodynamics, J. Geophys. Res.-Oceans, 118, 4169–4183, https://doi.org/10.1002/jgrc.20302, 2013.

Limaye, A. B., Adler, J. B., Moodie, A. J., Whipple, K. X., and Howard, A. D.: Effect of Standing Water on Formation of Fan-Shaped Sedimentary Deposits at Hypanis Valles, Mars, Geophys. Res. Lett., 50, e2022GL102367, https://doi.org/10.1029/2022GL102367, 2023.

Mahon, R., Hughes, C., Chen, H., and Shaw, J.: Ancient Channel-Mouth Bifurcation Angles on Earth and Mars, The Sedimentary Record, 22, https://doi.org/10.2110/001c.124824, 2024.

Malin, M. C. and Edgett, K. S.: Evidence for Persistent Flow and Aqueous Sedimentation on Early Mars, Science, https://doi.org/10.1126/science.1090544, 2015.

Martin, H. K. and Edmonds, D. A.: Avulsion dynamics determine fluvial fan morphology in a cellular model, Geology, 51, 796–800, https://doi.org/10.1130/G51138.1, 2023.

Mendenhall, W., Beaver, R. J., and Beaver, B. M.: Introduction to Probability and Statistics, Brooks/Cole, ISBN 0871500469, 2012.

Mohrig, D., Heller, P. L., Paola, C., and Lyons, W. J.: Interpreting avulsion process from ancient alluvial sequences: Guadalope-Matarranya system (northern Spain) and Wasatch Formation (western Colorado), Geol. Soc. Am. Bull., 112, 1787–1803, https://doi.org/10.1130/0016-7606(2000)112<1787:IAPFAA>2.0.CO;2, 2000.

Morais, E. S. and Montanher, O. C.: Avulsion in a meandering river: floodplain conditions for occurrence and effects in the parent channel, CATENA, 214, 106236, https://doi.org/10.1016/j.catena.2022.106236, 2022.

Morón, S., Amos, K., Edmonds, D. A., Payenberg, T., Sun, X., and Thyer, M.: Avulsion triggering by El Niño–Southern Oscillation and tectonic forcing: The case of the tropical Magdalena River, Colombia, GSA Bulletin, 129, 1300–1313, https://doi.org/10.1130/B31580.1, 2017.

Moscariello, A.: Alluvial fans and fluvial fans at the margins of continental sedimentary basins: geomorphic and sedimentological distinction for geo-energy exploration and development, SP, 440, 215–243, https://doi.org/10.1144/SP440.11, 2018.

Nichols, G. J.: Structural Controls on Fluvial Distributary Systems – The Luna System, Northern Spain, in: Recent developments in fluvial sedimentology, edited by: Ethridge, F. G., Flores, R. M., and Harvey, M. D., SEPM Society for Sedimentary Geology, https://doi.org/10.2110/pec.87.39.0269, 1987.

Nichols, G. J. and Fisher, J. A.: Processes, facies and architecture of fluvial distributary system deposits, Sediment. Geol., 195, 75–90, https://doi.org/10.1016/j.sedgeo.2006.07.004, 2007.

Nienhuis, J. H., Ashton, A. D., and Giosan, L.: What makes a delta wave-dominated?, Geology, 43, 511–514, https://doi.org/10.1130/G36518.1, 2015.

Nienhuis, J. H., Hoitink, A. J. F. T., and Törnqvist, T. E.: Future Change to Tide-Influenced Deltas, Geophys. Res. Lett., 45, 3499–3507, https://doi.org/10.1029/2018GL077638, 2018.

Nienhuis, J. H., Ashton, A. D., Edmonds, D. A., Hoitink, A. J. F., Kettner, A. J., Rowland, J. C., and Törnqvist, T. E.: Global-scale human impact on delta morphology has led to net land area gain, Nature, 577, 514–518, https://doi.org/10.1038/s41586-019-1905-9, 2020.

North, C. P. and Warwick, G. L.: Fluvial Fans: Myths, Misconceptions, and the End of the Terminal-Fan Model, J. Sediment. Res., 77, 693–701, https://doi.org/10.2110/jsr.2007.072, 2007.

Olariu, C. and Bhattacharya, J. P.: Terminal distributary channels and delta front architecture of river-dominated delta systems, J. Sediment. Res., 76, 212–233, https://doi.org/10.2110/jsr.2006.026, 2006.

Ori, G. G., Marinangeli, L., and Baliva, A.: Terraces and Gilbert-type deltas in crater lakes in Ismenius Lacus and Memnonia (Mars), J. Geophys. Res., 105, 17629–17641, https://doi.org/10.1029/1999JE001219, 2000.

Owen, A., Nichols, G. J., Hartley, A. J., Weissmann, G. S., and Scuderi, L. A.: Quantification of a Distributive Fluvial System: The Salt Wash DFS of the Morrison Formation, SW U.S.A., J. Sediment. Res., 85, 544–561, https://doi.org/10.2110/jsr.2015.35, 2015.

Paniagua-Arroyave, J. F. and Nienhuis, J. H.: The Quantified Galloway Ternary Diagram of Delta Morphology, J. Geophys. Res.-Earth, 129, e2024JF007878, https://doi.org/10.1029/2024JF007878, 2024.

Paola, C., Twilley, R. R., Edmonds, D. A., Kim, W., Mohrig, D., Parker, G., Viparelli, E., and Voller, V. R.: Natural Processes in Delta Restoration: Application to the Mississippi Delta, Annu. Rev. Mar. Sci., 3, 67–91, https://doi.org/10.1146/annurev-marine-120709-142856, 2011.

Parker, G., Paola, C., Whipple, K. X., and Mohrig, D.: Alluvial Fans Formed by Channelized Fluvial and Sheet Flow. I: Theory, J. Hydraul. Eng., 124, 985–995, https://doi.org/10.1061/(ASCE)0733-9429(1998)124:10(985), 1998.

Passalacqua, P.: The Delta Connectome: A network-based framework for studying connectivity in river deltas, Geomorphology, 277, 50–62, https://doi.org/10.1016/j.geomorph.2016.04.001, 2017.

Pearson, S. G., Van Prooijen, B. C., Elias, E. P. L., Vitousek, S., and Wang, Z. B.: Sediment Connectivity: A Framework for Analyzing Coastal Sediment Transport Pathways, J. Geophys. Res.-Earth, 125, e2020JF005595, https://doi.org/10.1029/2020JF005595, 2020.

Piliouras, A., Lauzon, R., and Rowland, J. C.: Unraveling the Combined Effects of Ice and Permafrost on Arctic Delta Morphodynamics, J. Geophys. Res.-Earth, 126, e2020JF005706, https://doi.org/10.1029/2020JF005706, 2021.

Pizzuto, J. E.: Sediment diffusion during overbank flows, Sedimentology, 34, 301–317, https://doi.org/10.1111/j.1365-3091.1987.tb00779.x, 1987.

Plink-Björklund, P.: Distributive Fluvial Systems: Fluvial and Alluvial Fans, in: Encyclopedia of Geology, Elsevier, 745–758, https://doi.org/10.1016/B978-0-08-102908-4.00015-1, 2021.

Radebaugh, J., Ventra, D., Lorenz, R. D., Farr, T., Kirk, R., Hayes, A., Malaska, M. J., Birch, S., Liu, Z. Y.-C., Lunine, J., Barnes, J., Le Gall, A., Lopes, R., Stofan, E., Wall, S., and Paillou, P.: Alluvial and fluvial fans on Saturn's moon Titan reveal processes, materials and regional geology, SP, 440, 281–305, https://doi.org/10.1144/SP440.6, 2018.

Rahman, M. M., Howell, J. A., and MacDonald, D. I. M.: Quantitative analysis of crevasse-splay systems from modern fluvial settings, J. Sediment. Res., 92, 751–774, https://doi.org/10.2110/jsr.2020.067, 2022.

Reitz, M. D. and Jerolmack, D. J.: Experimental alluvial fan evolution: Channel dynamics, slope controls, and shoreline growth, J. Geophys. Res., 117, 2011JF002261, https://doi.org/10.1029/2011JF002261, 2012.

Saito, Y., Thanawat, J., Chaimanee, N., Jarupongsakul, T., and Syvitski, J. P. M.: Shrinking Megadeltas in Asia: Sea-level Rise and Sediment Reduction Impacts from Case Study of the Chao Phraya Delta, Inprint Newsletter of the IGBP/IHDP Land Ocean Interaction in the Coastal Zone, 3–9, https://www.researchgate.net/profile/Yoshiki-Saito/publication/234045413_Shrinking_Megadeltas_in_Asia_Sea-level_Rise_and_Sediment_Reduction_Impacts_from_Case_Study_of_the_Chao_Phraya_Delta/links/02bfe50e829eab7e2a000000/Shrinking-Megadeltas-in-Asia-Sea-level-Rise-and-Sediment-Reduction-Impacts-from-Case-Study-of-the-Chao-Phraya-Delta.pdf (last access: 6 May 2025), 2007.

Schumm, S. A.: The fluvial system, Food and Agriculture Organization of the United Nations, Wiley, ISBN 978-0471019015, 1977.

Schwanghart, W. and Kuhn, N. J.: TopoToolbox: A set of Matlab functions for topographic analysis, Environ. Modell. Softw., 25, 770–781, https://doi.org/10.1016/j.envsoft.2009.12.002, 2010.

Seybold, H., Andrade, J. S., and Herrmann, H. J.: Modeling river delta formation, P. Natl. Acad. Sci. USA, 104, 16804–16809, https://doi.org/10.1073/pnas.0705265104, 2007.

Seybold, H., Rothman, D. H., and Kirchner, J. W.: Climate's watermark in the geometry of stream networks, Geophys. Res. Lett., 44, 2272–2280, https://doi.org/10.1002/2016GL072089, 2017.

Seybold, H. J., Kite, E., and Kirchner, J. W.: Branching geometry of valley networks on Mars and Earth and its implications for early Martian climate, Sci. Adv., 4, eaar6692, https://doi.org/10.1126/sciadv.aar6692, 2018.

Shaw, J. B., Miller, K., and McElroy, B.: Island Formation Resulting From Radially Symmetric Flow Expansion, J. Geophys. Res.-Earth, 123, 363–383, https://doi.org/10.1002/2017JF004464, 2018.

Singh, H., Parkash, B., and Gohain, K.: Facies analysis of the Kosi megafan deposits, Sediment. Geol., 85, 87–113, https://doi.org/10.1016/0037-0738(93)90077-I, 1993.

Sinha, R.: The Great avulsion of Kosi on 18 August 2008, Current Science, 97, 429–433, 2009.

Slingerland, R. and Smith, N. D.: Necessary conditions for a meandering-river avulsion, Geology, 26, 435–438, https://doi.org/10.1130/0091-7613(1998)026<0435:NCFAMR>2.3.CO;2, 1998.

Slingerland, R. and Smith, N. D.: River avulsions and their deposits, Annu. Rev. Earth Planet. Sci., 32, 257–285, https://doi.org/10.1146/annurev.earth.32.101802.120201, 2004.

Smart, J. S. and Moruzzi, V. L.: Quantitative properties of delta channel networks, IBM Thomas J. Watson Research Center, https://apps.dtic.mil/sti/html/tr/AD0719918/ (last access: 8 May 2025), 1971.

Syvitski, J. P. M. and Brakenridge, G. R.: Causation and avoidance of catastrophic flooding along the Indus River, Pakistan, GSA Today, 23, 4–10, https://doi.org/10.1130/GSATG165A.1, 2013.

Syvitski, J. P. M., Kettner, A. J., Overeem, I., Hutton, E. W. H., Hannon, M. T., Brakenridge, G. R., Day, J., Vörösmarty, C., Saito, Y., Giosan, L., and Nicholls, R. J.: Sinking deltas due to human activities, Nat. Geosci., 2, 681–686, https://doi.org/10.1038/ngeo629, 2009.

Tebolt, M. and Goudge, T. A.: Global investigation of martian sedimentary fan features: Using stratigraphic analysis to study depositional environment, Icarus, 372, 114718, https://doi.org/10.1016/j.icarus.2021.114718, 2022.

Tejedor, A., Longjas, A., Zaliapin, I., and Foufoula-Georgiou, E.: Delta channel networks: 1. A graph-theoretic approach for studying connectivity and steady state transport on deltaic surfaces, Water Resour. Res., 51, 3998–4018, https://doi.org/10.1002/2014WR016577, 2015.

Tejedor, A., Longjas, A., Edmonds, D. A., Zaliapin, I., Georgiou, T. T., Rinaldo, A., and Foufoula-Georgiou, E.: Entropy and optimality in river deltas, P. Natl. Acad. Sci. USA, 114, 11651–11656, https://doi.org/10.1073/pnas.1708404114, 2017.

Törnqvist, T. E. and Bridge, J. S.: Spatial variation of overbank aggradation rate and its influence on avulsion frequency, Sedimentology, 49, 891–905, https://doi.org/10.1046/j.1365-3091.2002.00478.x, 2002.

Trampush, S. M. and Hajek, E. A.: Preserving proxy records in dynamic landscapes: Modeling and examples from the Paleocene-Eocene Thermal Maximum, Geology, 45, 967–970, https://doi.org/10.1130/G39367.1, 2017.

Trauth, M. H.: MATLAB® Recipes for Earth Sciences, Springer, https://doi.org/10.1007/978-3-031-57949-3, 2006.

Ventra, D. and Clarke, L. E.: Geology and geomorphology of alluvial and fluvial fans: current progress and research perspectives, SP, 440, 1–21, https://doi.org/10.1144/SP440.16, 2018.

Virtanen, P., Gommers, R., Oliphant, T. E., Haberland, M., Reddy, T., Cournapeau, D., Burovski, E., Peterson, P., Weckesser, W., Bright, J., van der Walt, S. J., Brett, M., Wilson, J., Millman, K. J., Mayorov, N., Nelson, A. R. J., Jones, E., Kern, R., Larson, E., Carey, C. J., Polat, İ., Feng, Y., Moore, E. W., VanderPlas, J., Laxalde, D., Perktold, J., Cimrman, R., Henriksen, I., Quintero, E. A., Harris, C. R., Archibald, A. M., Ribeiro, A. H., Pedregosa, F., van Mulbregt, P., and SciPy 1.0 Contributors: SciPy 1.0: fundamental algorithms for scientific computing in Python, Nat. Methods, 17, 261–272, https://doi.org/10.1038/s41592-019-0686-2, 2020.

Vulis, L., Tejedor, A., Ma, H., Nienhuis, J. H., Broaddus, C. M., Brown, J., Edmonds, D. A., Rowland, J. C., and Foufoula-Georgiou, E.: River Delta Morphotypes Emerge From Multiscale Characterization of Shorelines, Geophys. Res. Lett., 50, e2022GL102684, https://doi.org/10.1029/2022GL102684, 2023.

Walker, H. J.: Arctic Deltas, J. Coast. Res., 14, 718–738, 1998.

Wall, S., Hayes, A., Bristow, C., Lorenz, R., Stofan, E., Lunine, J., Le Gall, A., Janssen, M., Lopes, R., Wye, L., Soderblom, L., Paillou, P., Aharonson, O., Zebker, H., Farr, T., Mitri, G., Kirk, R., Mitchell, K., Notarnicola, C., Casarano, D., and Ventura, B.: Active shoreline of Ontario Lacus, Titan: A morphological study of the lake and its surroundings, Geophys. Res. Lett., 37, L05202, https://doi.org/10.1029/2009GL041821, 2010.

Wang, J. and Plink-Björklund, P.: Stratigraphic complexity in fluvial fans: Lower Eocene Green River Formation, Uinta Basin, USA, Basin Res., 31, 892–919, https://doi.org/10.1111/bre.12350, 2019.

Waskom, M.: seaborn: statistical data visualization, Journal of Open Source Software, 6, 3021, https://doi.org/10.21105/joss.03021, 2021.

Weissmann, G. S., Hartley, A. J., Nichols, G. J., Scuderi, L. A., Olson, M., Buehler, H., and Banteah, R.: Fluvial form in modern continental sedimentary basins: Distributive fluvial systems, Geology, 38, 39–42, https://doi.org/10.1130/G30242.1, 2010.

Weissmann, G. S., Hartley, A. J., Scuderi, L. A., Nichols, G. J., Davidson, S. K., Owen, A., Atchley, S. C., Bhattacharyya, P., Chakraborty, T., Ghosh, P., Nordt, L. C., Michel, L., and Tabor, N. J.: Prograding distributive fluvial systems–geomorphic models and ancient examples, SEPM Special Publication 104, https://doi.org/10.2110/sepmsp.104.16, 2013.

Weissmann, G. S., Hartley, A. J., Scuderi, L. A., Nichols, G. J., Owen, A., Wright, S., Felicia, A. L., Holland, F., and Anaya, F. M. L.: Fluvial geomorphic elements in modern sedimentary basins and their potential preservation in the rock record: A review, Geomorphology, 250, 187–219, https://doi.org/10.1016/j.geomorph.2015.09.005, 2015.

Witek, P. P. and Czechowski, L.: Dynamical modelling of river deltas on Titan and Earth, Planet. Space Sci., 105, 65–79, https://doi.org/10.1016/j.pss.2014.11.005, 2015.

Wolinsky, M. A., Edmonds, D. A., Martin, J., and Paola, C.: Delta allometry: Growth laws for river deltas, Geophys. Res. Lett., 37, 2010GL044592, https://doi.org/10.1029/2010GL044592, 2010.

Wood, L. J.: Quantitative geomorphology of the Mars Eberswalde delta, Geol. Soc. Am. Bull., 118, 557–566, https://doi.org/10.1130/B25822.1, 2006.

Wright, L. D.: Sediment transport and deposition at river mouths: A synthesis, Geol. Soc. Am. Bull., 88, 857, https://doi.org/10.1130/0016-7606(1977)88<857:STADAR>2.0.CO;2, 1977.

Xu, Z. and Plink-Björklund, P.: Quantifying Formative Processes in River- and Tide-Dominated Deltas for Accurate Prediction of Future Change, Geophys. Res. Lett., 50, e2023GL104434, https://doi.org/10.1029/2023GL104434, 2023.

Yang, H.: Numerical investigation of avulsions in gravel-bed braided rivers, Hydrol. Process., 34, 3702–3717, https://doi.org/10.1002/hyp.13837, 2020.